FROM ELECTROSPINNING TO THERMAL MANAGEMENT IN MICROELECTRONICS, FROM CO-ELECTROSPINNING TO NANOFLUIDICS

Center of Smart Interfaces

TECHNISCHE UNIVERSITÄT DARMSTADT

A.L. Yarin

Mechanical & Industrial Engineering

University of Illinois at Chicago,U.S.A., and TU Darmstadt, Germany

Supported in part in 2006-2011 by:

NSF: NIRT CBET-0609062,
NSF: NER-CBET 0708711,
NSF: CBET-0966764,
NASA: NNX10AR99G
The Volkswagen Foundation

Acknowledgements:

PhD Students: Suman Sinha Ray (UIC)
Raman Srikar (UIC)
Yiyun Zhang (UIC)
Andreas Lembach (TUD)
C. M. Weickgenannt (TUD)
Collaborators: Dr. A.V. Bazilevsky (UIC)
Dr. I.V. Roisman (TUD)
Dr. T. Gambaryan-Roisman (TUD)
Dr. C. Tropea (TUD)
Dr. P. Stephan (TUD)
Dr. J. Yagoobi (IIT)

Mechanical & Industrial Engineering

Outline

1. Electrospinning of nanofiber mats
2. Drops on nanofiber mats: static superhydrophobicity
3. Drop impact on nanofiber mats: dynamic wettability
4. Cooling of micro- and opto-electronics, and radiological devices; UAVs, UGVs and server racks
5. Carbon nanotubes via co-electrospinning
6. Carbon nanotubes from a single nozzle
7. Pressure-driven nanofluidics in macroscopically long carbon nanotubes
8. Template approach: nanotube strips
9. Beyond Poiseuille

Mechanical & Industrial Engineering

Electrospinning Setup

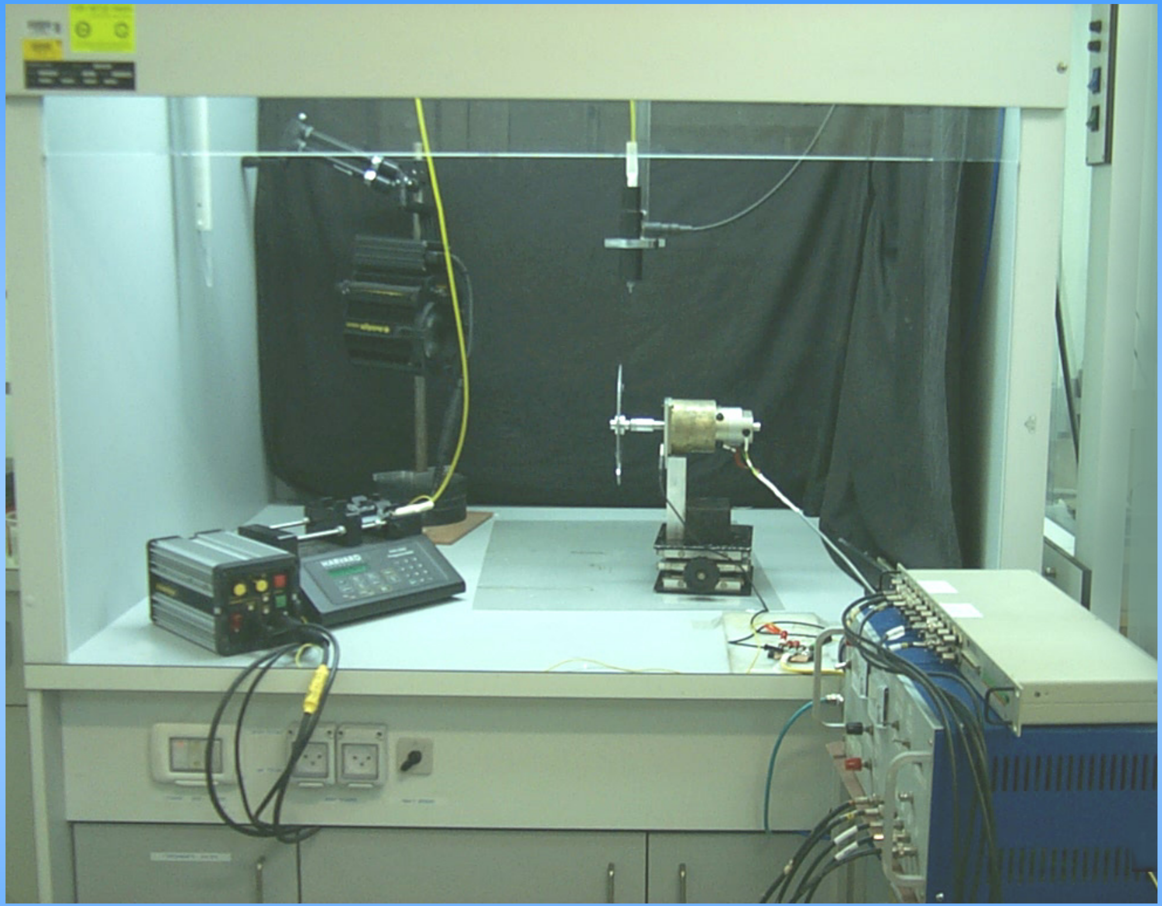

Mechanical & Industrial Engineering

Process Initiation: Taylor Cone

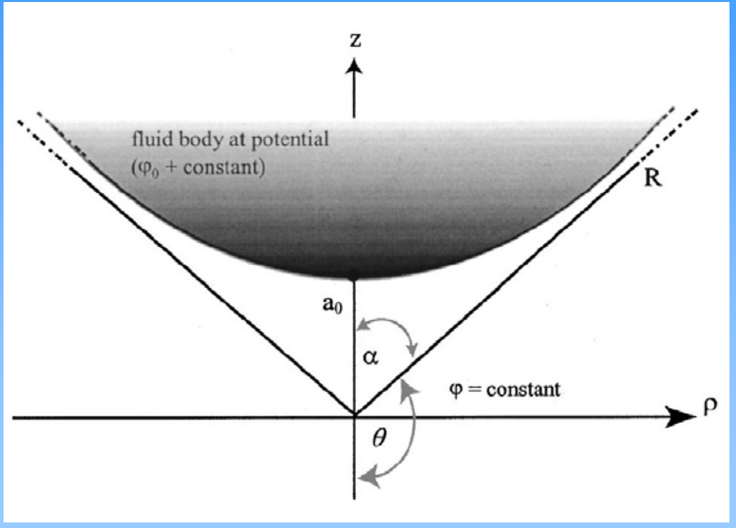

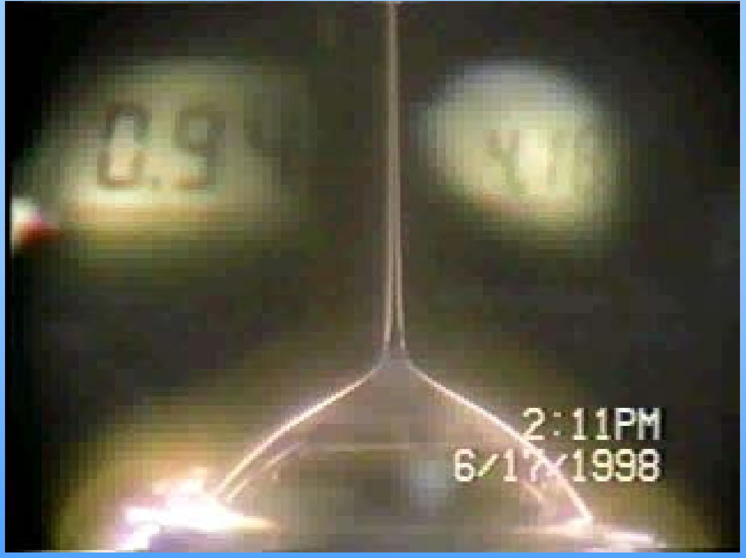

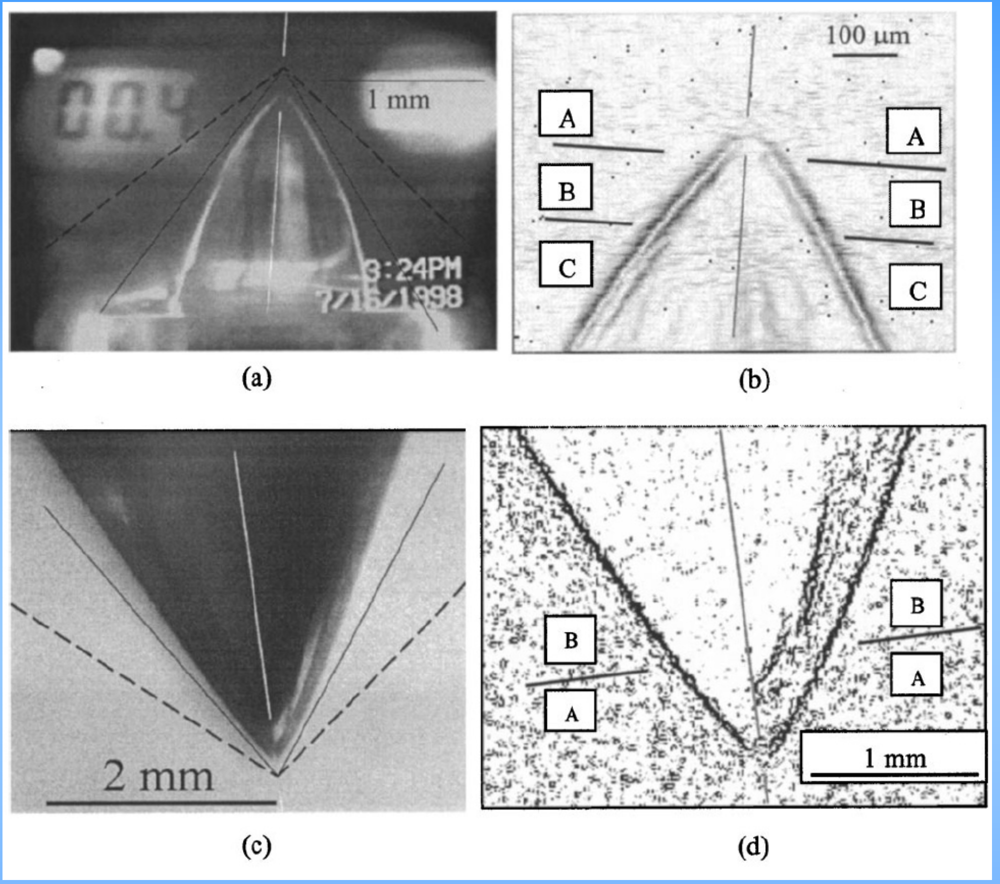

Mechanical & Industrial Engineering

Yarin A L, Reneker D H, Kombhongse S, *J. App. Phys*. 90, 2001

Electrospinning of Polymer Solutions

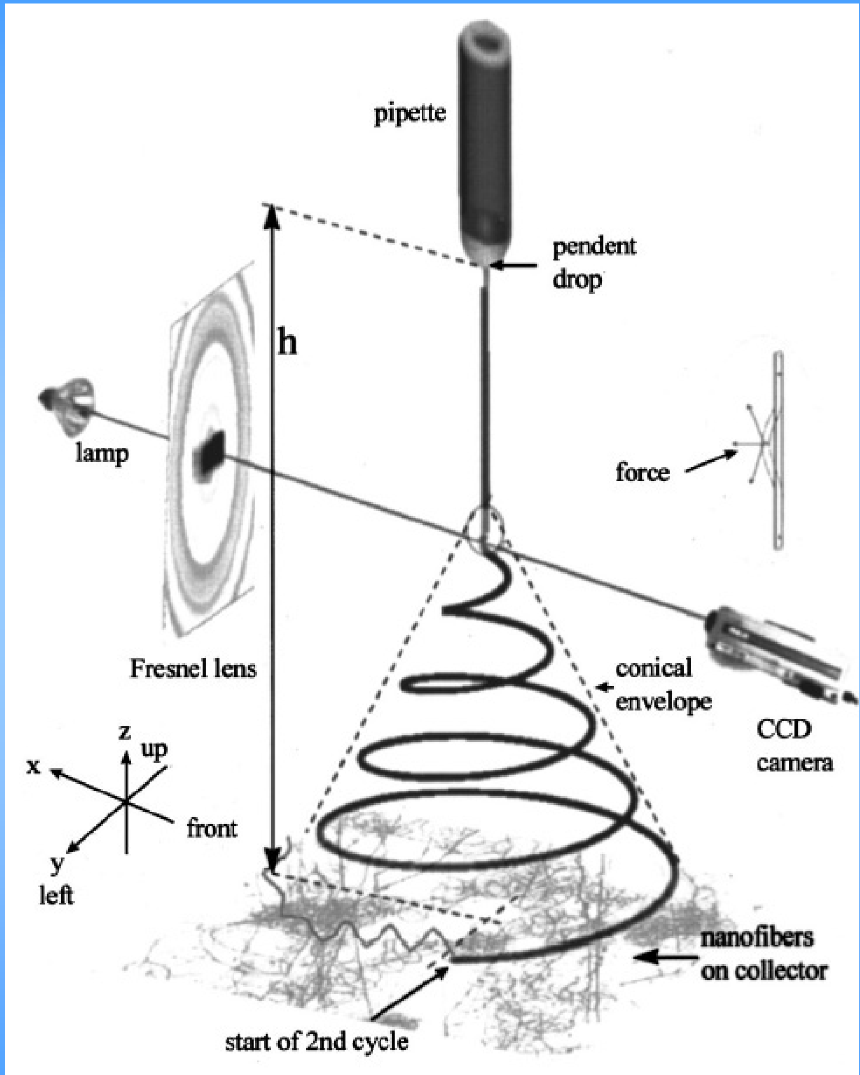

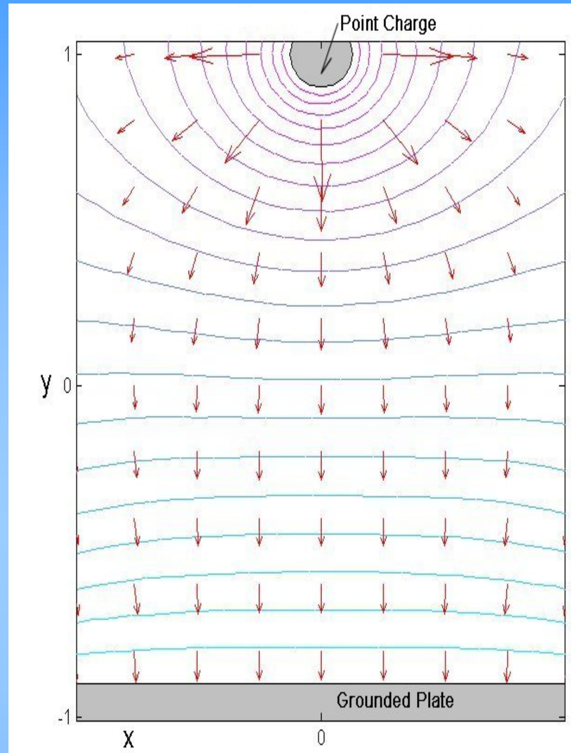

Reneker D H, Yarin A L, Fong H, Koombhongse S, *J. App. Phys.* 87, 2000

Yarin A L, Koombhongse S, Reneker D H, *J. App. Phys.* 89, 2001

Mechanical & Industrial Engineering

Electrospinning of Polymer Solutions

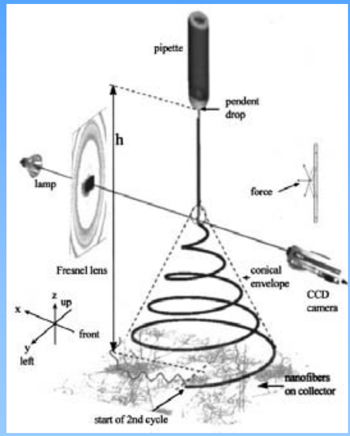

Mechanical & Industrial Engineering

Reneker, Yarin, Fong, Koombhogse

Electrospinning of Polymer Solutions

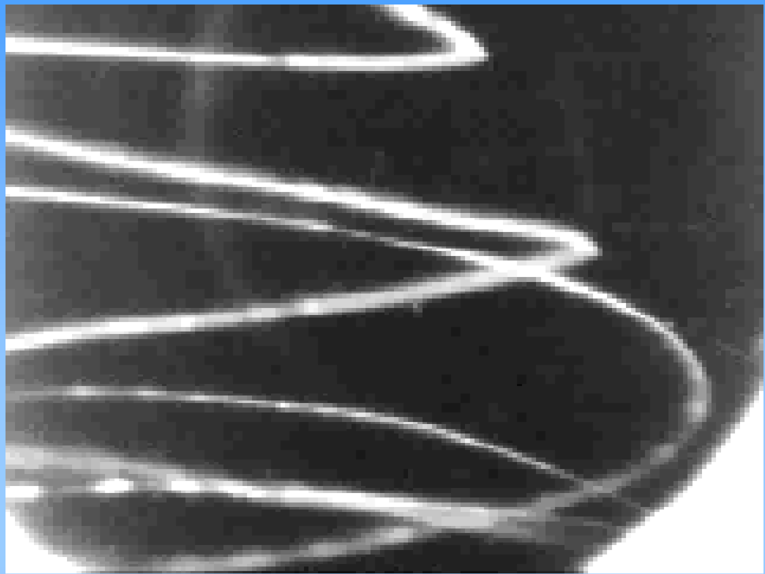

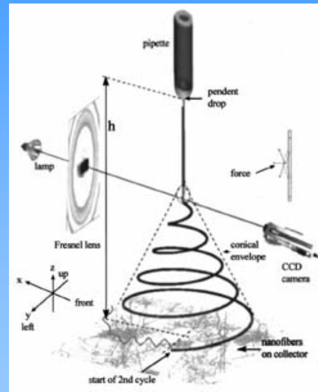

Reneker, Yarin, Fong, Koombhongse

Mechanical & Industrial Engineering

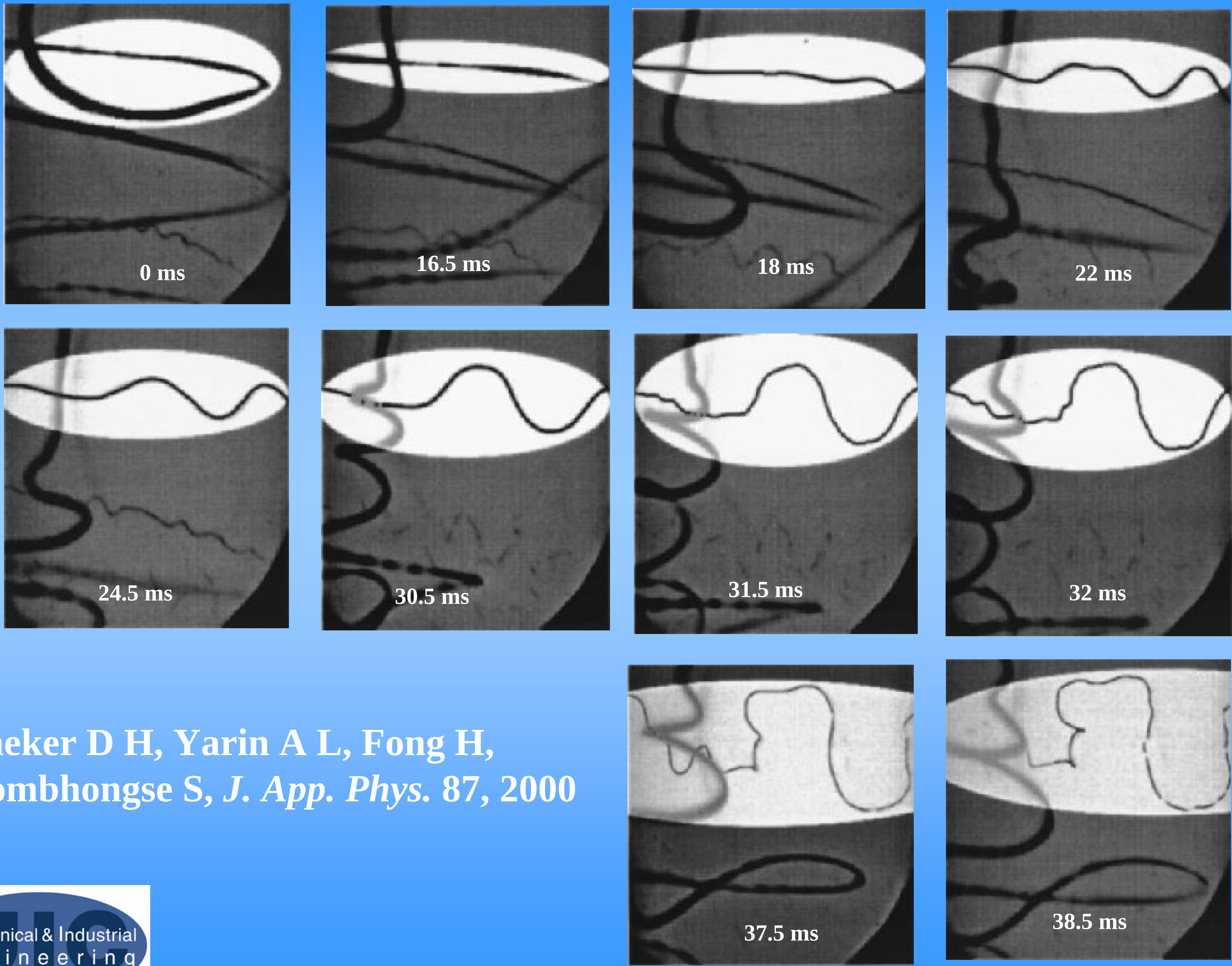

Reneker D H, Yarin A L, Fong H, Koombhongse S, *J. App. Phys.* 87, 2000

Drop Impact: Experimental Setups

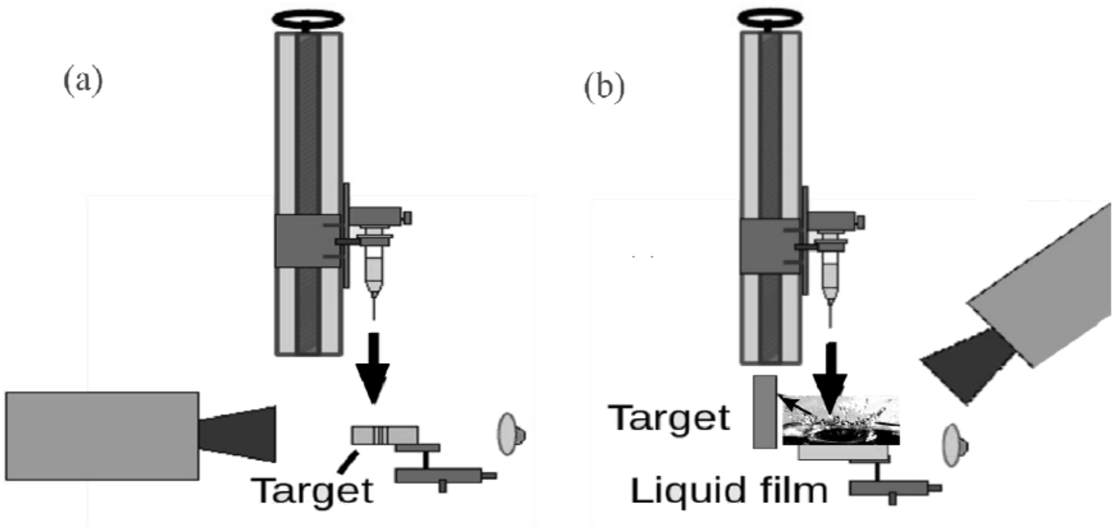

a- Syringe drop generator for direct impact of 2-3 mm or 100 micron drops at velocities of about 2 m/s.
b- Syringe drop generator produces primary drop, which impact on liquid film and produce corona splash to generate 0.4-1.4 mm drops for oblique impact.

Electrospun Nanofiber Mat and a Droplet Softly Deposited on it

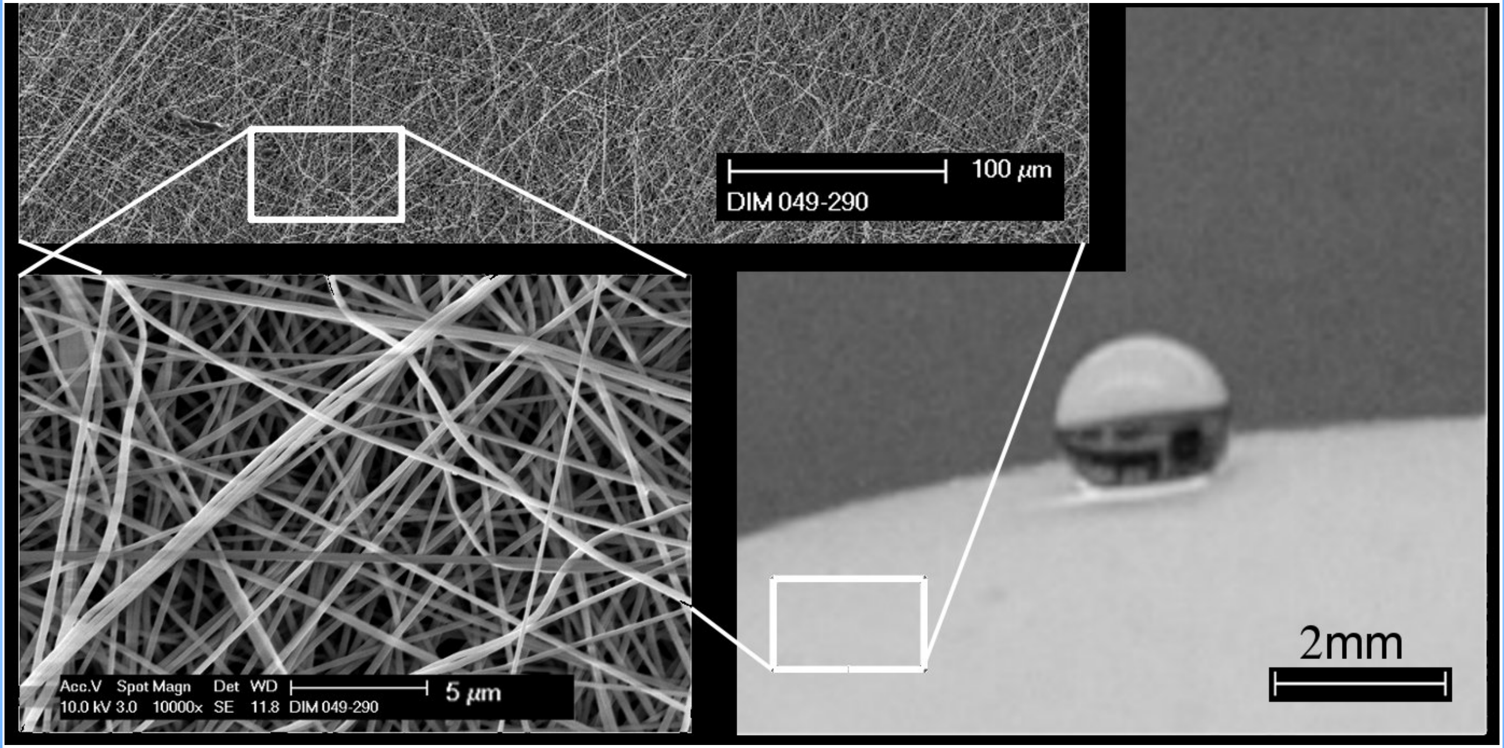

Static superhydrophobicity: Cassie-Baxter state due to 90-95% of air in the mat

A.Lembach, H.B. Tan, I.V. Roisman, T. Gambaryan-Roisman, Y. Zhang, C. Tropea, A.L. Yarin. Langmuir 26(12) 9516-9523 (2010).

Drop Impact on a Dry Solid Wall

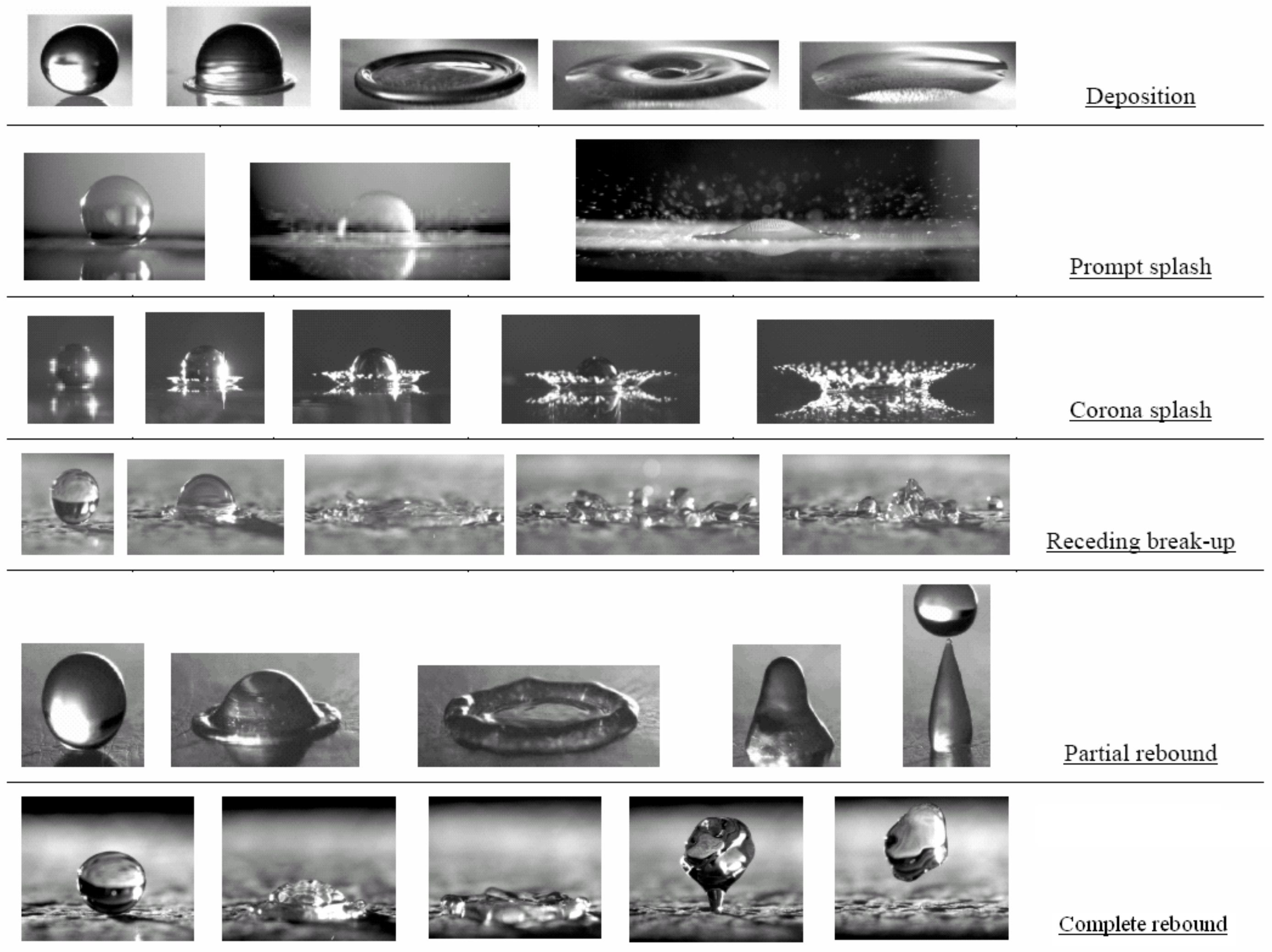

Mechanical & Industrial Engineering

Rioboo R, Tropea C, Marengo M. 2001. Outcomes from a drop impact on solid surfaces. *At. Sprays 11:155–65*

Drop Impact on a Dry Nanofiber Mat

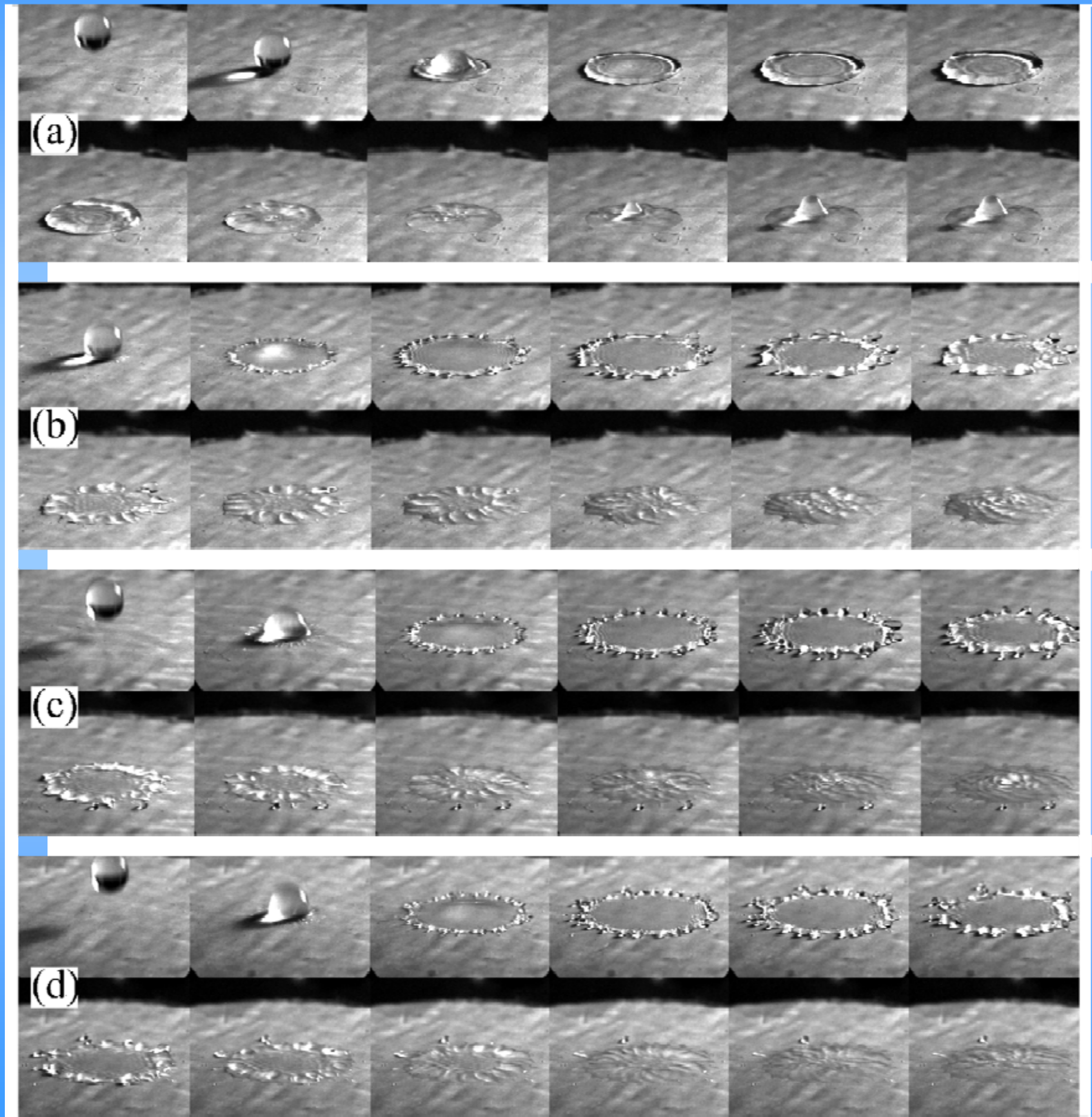

Contact line is pinned: no receding, no bouncing; Dynamically imposed Wenzel state

Drop Impact on Prewetted Nanofiber Mat: Back to Corona Splash

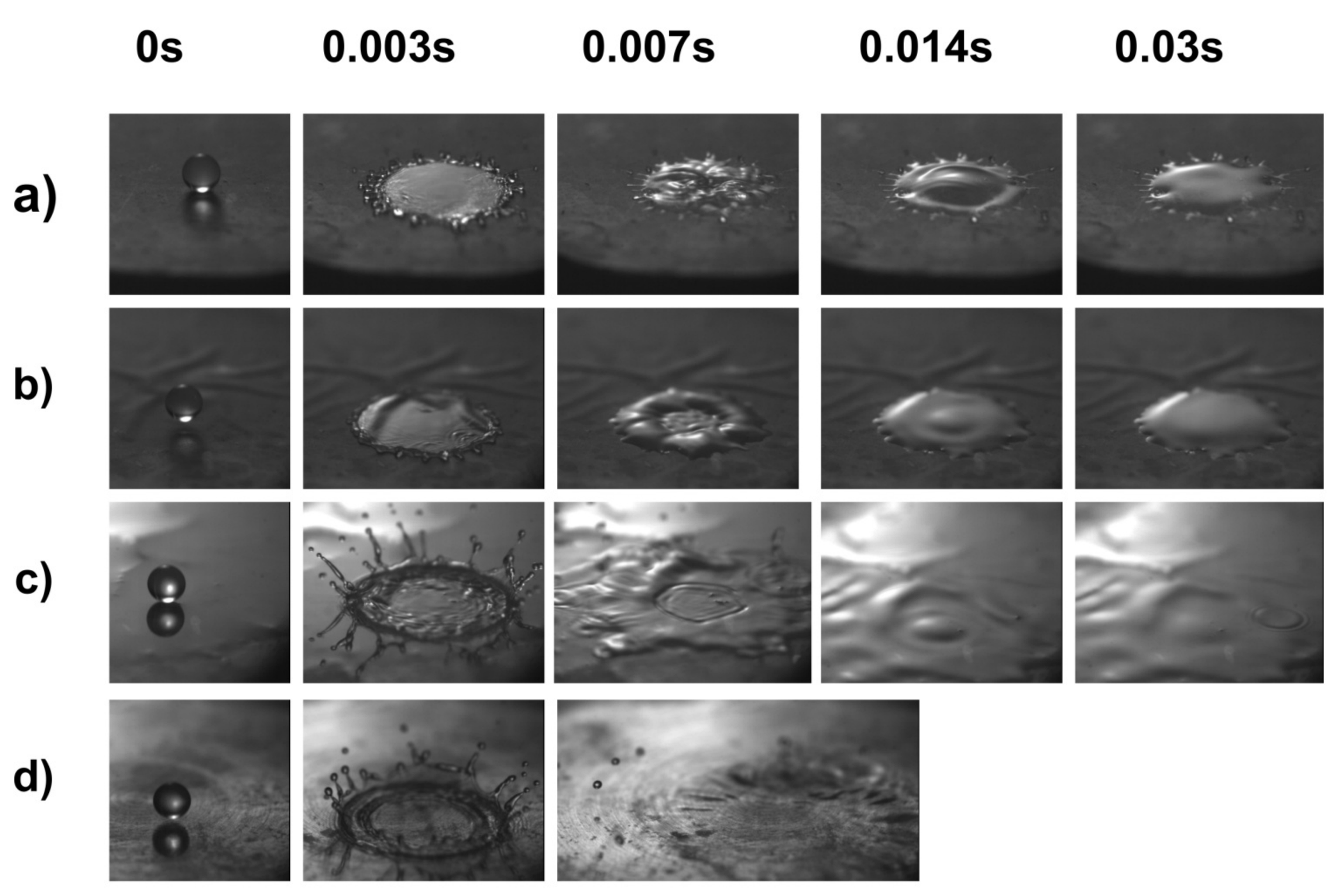

Mechanical & Industrial Engineering

Accumulation and Channeling of Kinetic Energy in Drop Impact on a Pore

Pressure impulse and potential

$$\Pi = \lim_{\substack{\tau\to 0\\ p\to\infty}} \int_0^\tau \Delta p\,dt; \quad \varphi = -\Pi/\rho$$

Potential φ is a harmonic function

Evaluating pressure impulse

Compressible impact:

The convective part of the force:

$$F_c = \rho V_0 c D^2$$

The "water hammer"– like part of the force:

$$F_{wh} = -\rho D^3 A = -\rho D^3\left(-V_0 c/D\right) = \rho V_0 c D^2.$$

Therefore,

$$\Delta p = F/D^2 = \rho V_0 c; \quad \tau = D/c, \text{ and}$$

$$\Pi = \rho V_0 D; \ \varphi_0 = -V_0 D$$

Mechanical & Industrial Engineering

Accumulation and Channeling of Kinetic Energy in Drop Impact on a Pore

Evaluating pressure impulse

Incompressible impact:

The convective part of the force:

$F_c = \rho V_0^2 D^2$

The "water hammer"– like part of the force:

$F_{wh} = -\rho D^3 A = -\rho D^3 \left(-V_0 V_0 / D\right) = \rho V_0^2 D^2.$

Therefore,

$\Delta p = F / D^2 = \rho V_0^2; \quad \tau = D / V_0$, and

$\Pi = \rho V_0 D; \ \varphi_0 = -V_0 D$ – as in the compressible case

Accumulation and Channeling of Kinetic Energy in Drop Impact on a Pore

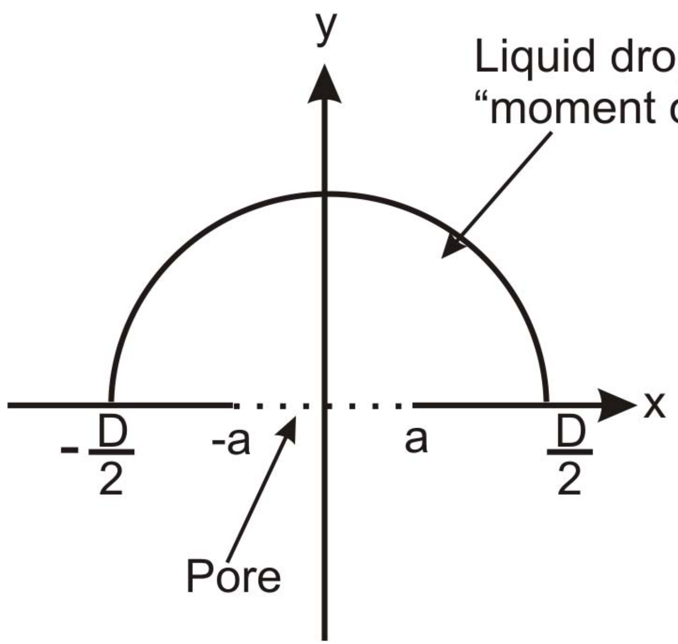

Mechanical & Industrial Engineering

Accumulation and Channeling of Kinetic Energy in Drop Impact on a Pore

The boundary condition for the harmonic potential: Planar case

$$\text{Over } -\infty \le X \le -a,\ y = 0;$$
$$\text{and over } a \le X \le \infty,\ y = 0 \text{ (2D wall)}:$$
$$\varphi(X) = \varphi_0 = -V_0 D$$
$$\text{Over } -a < X < a,\ y = 0 \text{ (2D pore)}:$$
$$\varphi(X) = 0.$$

Mechanical & Industrial Engineering

Accumulation and Channeling of Kinetic Energy in Drop Impact on a Pore

The harmonic potential in the liquid drop in the upper half-plane is given by the Cauchy formula, which reduces to Poisson's integral formula for the upper half-plane

$$\varphi(x,y) = \frac{1}{\pi}\int_{-\infty}^{\infty} \frac{\varphi(X,0)\,y}{(x-X)+y^2}\,dX = -\frac{\varphi_0}{\pi}\arctan\left(\frac{2ay}{x^2+y^2-a^2}\right)$$

Therefore,

$$v_{\text{opening}}(x) = \left.\frac{\partial\varphi}{\partial y}\right|_{y=0} = \frac{V_0 D}{\pi}\frac{2a}{x^2-a^2};$$

$$\left|v_{\text{opening}}(0)\right| = V_0\frac{2}{\pi}\frac{D}{a}; \quad a = d/2$$

Mechanical & Industrial Engineering

The Reasons of Filling Non-wettable Nanofiber Mats

Predicted penetration speed: accumulation and channeling of kinetic energy (a la shaped-charge jets!)

$$U = \frac{4}{\pi}\frac{D}{d}V_0$$

Impregnation: Lucas-Washburn speed

$$U_{LW} = \frac{\sigma d \cos\theta}{8\mu H}$$

$$\frac{D}{d} >> 1, \quad U >> U_{LW}$$

Wettability plays practically no role: it is possible to fill non-wettable pores!!!

Mechanical & Industrial Engineering

Accumulation and Channeling of Kinetic Energy in Drop Impact on a Pore

The boundary condition for the harmonic potential: Cylindrical case-Solved by the Fourier method as a problem with a continuous spectrum

$$\text{Over } a \le r \le \infty,\ z = 0 \text{ (2D wall)}:$$
$$\varphi(X) = \varphi_0 = -V_0 D$$
$$\text{Over } 0 \le t < a,\ y = 0 \text{ (2D pore)}:$$
$$\varphi(X) = 0.$$

C. M. Weickgenannt, Y. Zhang, A. N. Lembach, I.V. Roisman, T. Gambaryan, A.L. Yarin, C.Tropea, Phus. Rev. E. (2011).

Mechanical & Industrial Engineering

Accumulation and Channeling of Kinetic Energy in Drop Impact on a Pore

The harmonic potential in the liquid drop in the upper semi-space: Cylindrical case-solution as the Fourier-Bessel integral

$$\varphi(r,z) = V_0 D a \int_0^{\infty} J_0(\nu r) J_1(\nu a) \exp(-\nu z) d\nu$$

Therefore,

$$v_z(r)\Big|_{z=0} = \frac{\partial \varphi}{\partial z}\Big|_{z=0} = -\frac{V_0 D}{a} \int_0^{\infty} \xi J_0\left(\frac{r}{a}\xi\right) J_1(\xi) d\xi;$$

$$\left| v_z(r=0)\Big|_{z=0} \right| = V_0 \frac{2D}{d}; \quad a = d/2$$

Mechanical & Industrial Engineering

The Reasons of Filling Non-wettable Nanofiber Mats

Predicted penetration speed: Predicted in the cylindrical case

$$U = \frac{2D}{d} V_0$$

Even higher than in the planar case!

Wettability plays practically no role: it is possible to fill non-wettable pores!!!

Mechanical & Industrial Engineering

FC-7500: Millipede

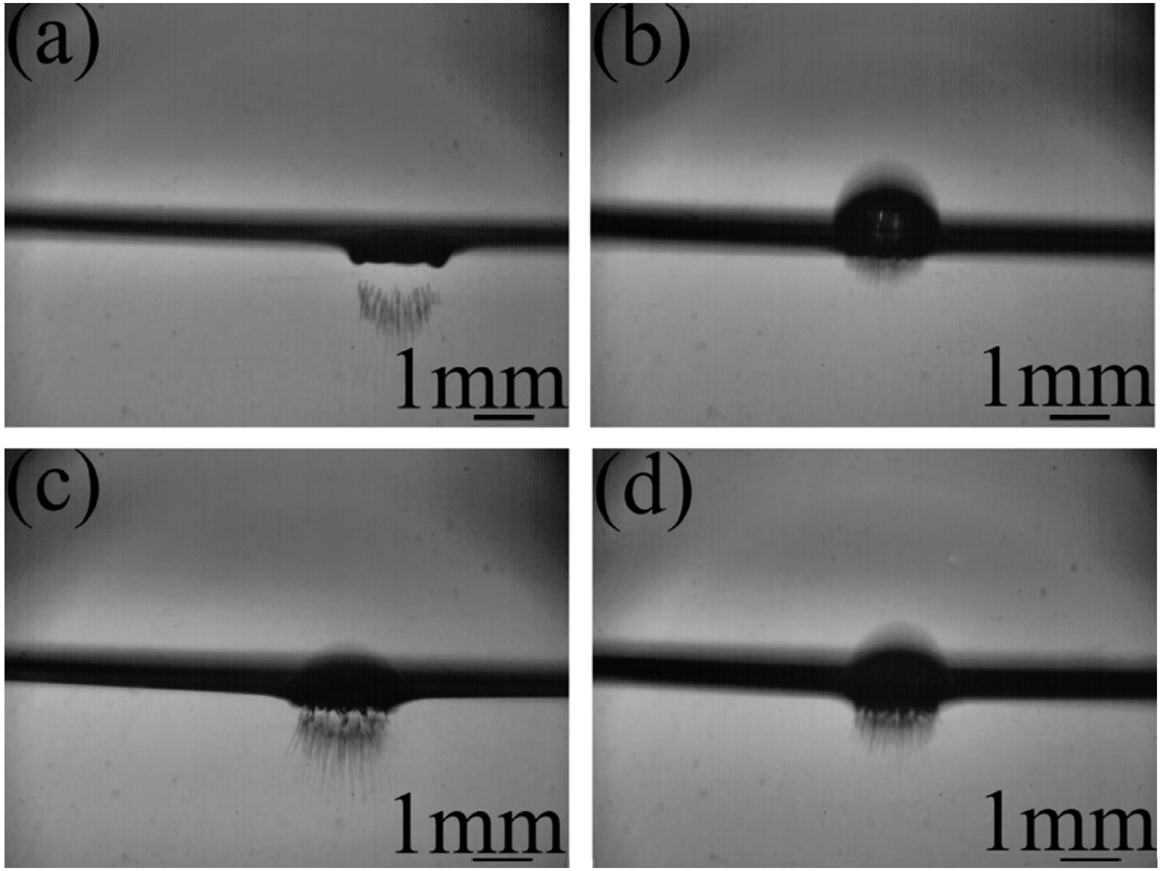

Mechanical & Industrial Engineering

Observations of Water Spreading inside Nanofiber Mats

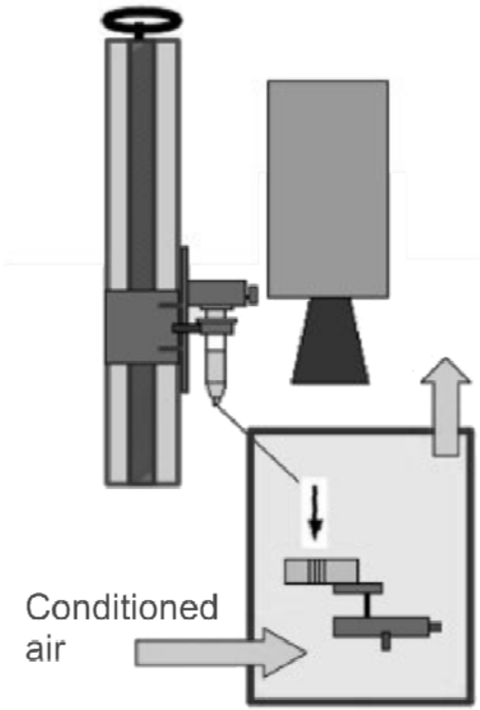

Setup for obervations of nanomat impregnation

Water Spreading inside Nanofiber Mat: Experimental Results

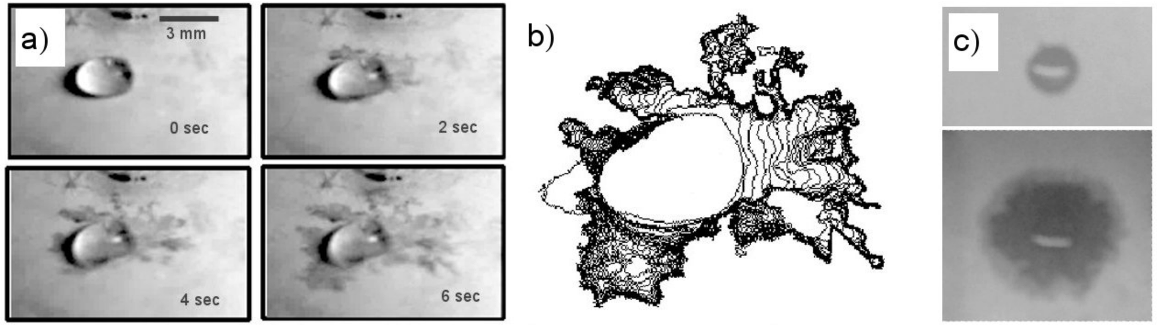

Matching of refractive indexes of wet nanofibers and water makes the copper substrate visible

Mechanical & Industrial Engineering

Water Spreading inside Nanofiber Mat: 1D Axisymmetric Theory

The moisture transport equation:

$$\frac{\partial u}{\partial t} = a_m \frac{1}{r}\frac{\partial}{\partial r}\left(r \frac{\partial u}{\partial r} \right)$$

The initial and boundary conditions:

$$t = 0: \;\; u = \chi(r); \;\; t \geq 0: \;\; u < \infty, \;\; r = 0 \;\; \text{and} \;\; u = 0, \;\; r = \infty$$

The solution:

$$u(r,t) = \frac{1}{2a_m t} \exp\left(-\frac{r^2}{4a_m t} \right) \int_0^{D/2} \exp\left(-\frac{\xi^2}{4a_m t} \right) I_0\left(\frac{r\xi}{2a_m t} \right) \xi \, d\xi$$

Mechanical & Industrial Engineering

Water Spreading inside Nanofiber Mat: 1D Axisymmetric Theory

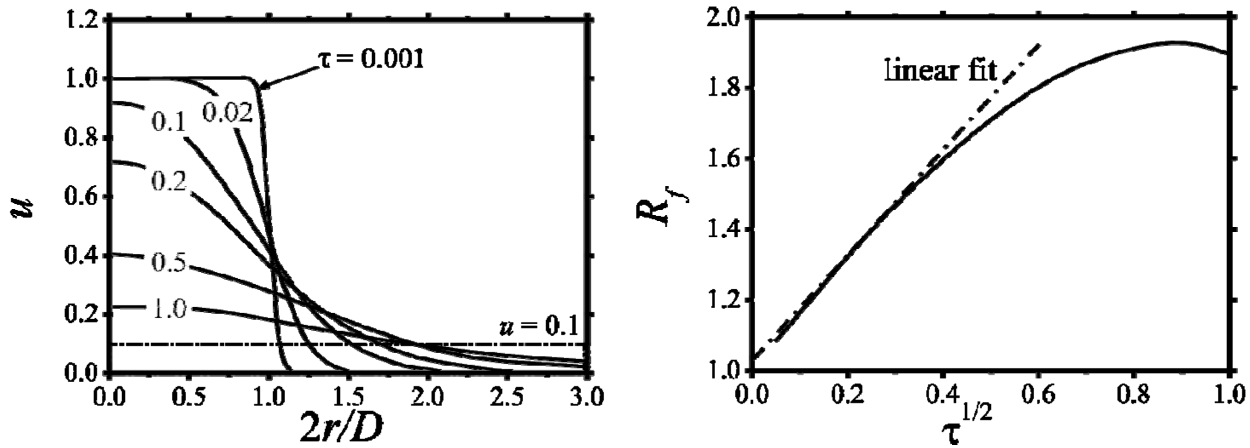

Water Spreading inside Nanofiber Mat: Experiments vs. Theory

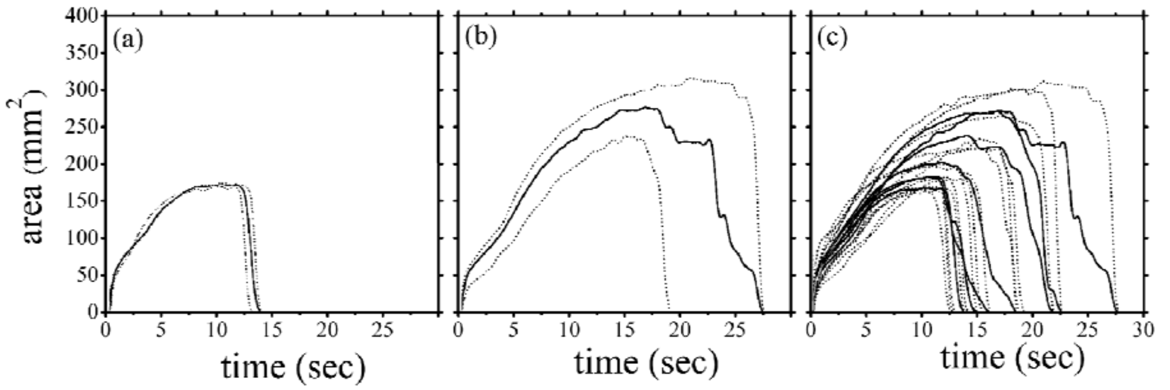

$$R_f = 1.492\sqrt{a_m t} + \text{const}$$

The moisture transport coefficient:

$$a_m = 8 \times 10^{-4}\,\text{cm}^2/\text{s}$$

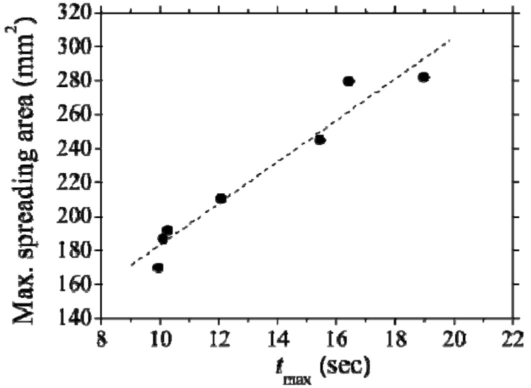

Microelectronics Miniaturization: UAV-Unmanned Aerial Vehicles

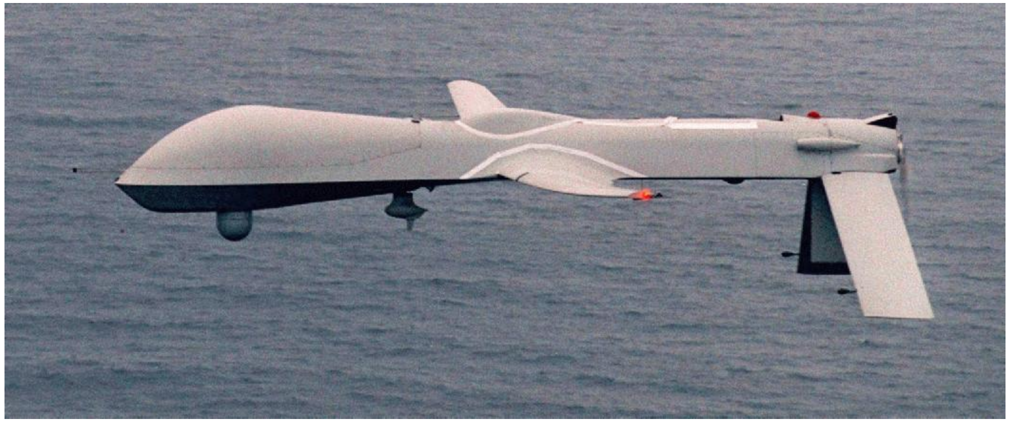

The images were downloaded from internet

Microelectronics Miniaturization: UGV-Unmanned Ground Vehicles Searching for Hazardous Chemicals

“Griffon: A Man-Portable Hybrid UGV/UAV,” Brian Yamauchi and Pavlo Rudakevych, *Industrial Robot, vol. 31, no. 5, pp. 443-450, 2004.*

Drop/Spray Cooling through Nanofiber Mats: Thermal Stability? PCL Easily Shrinks

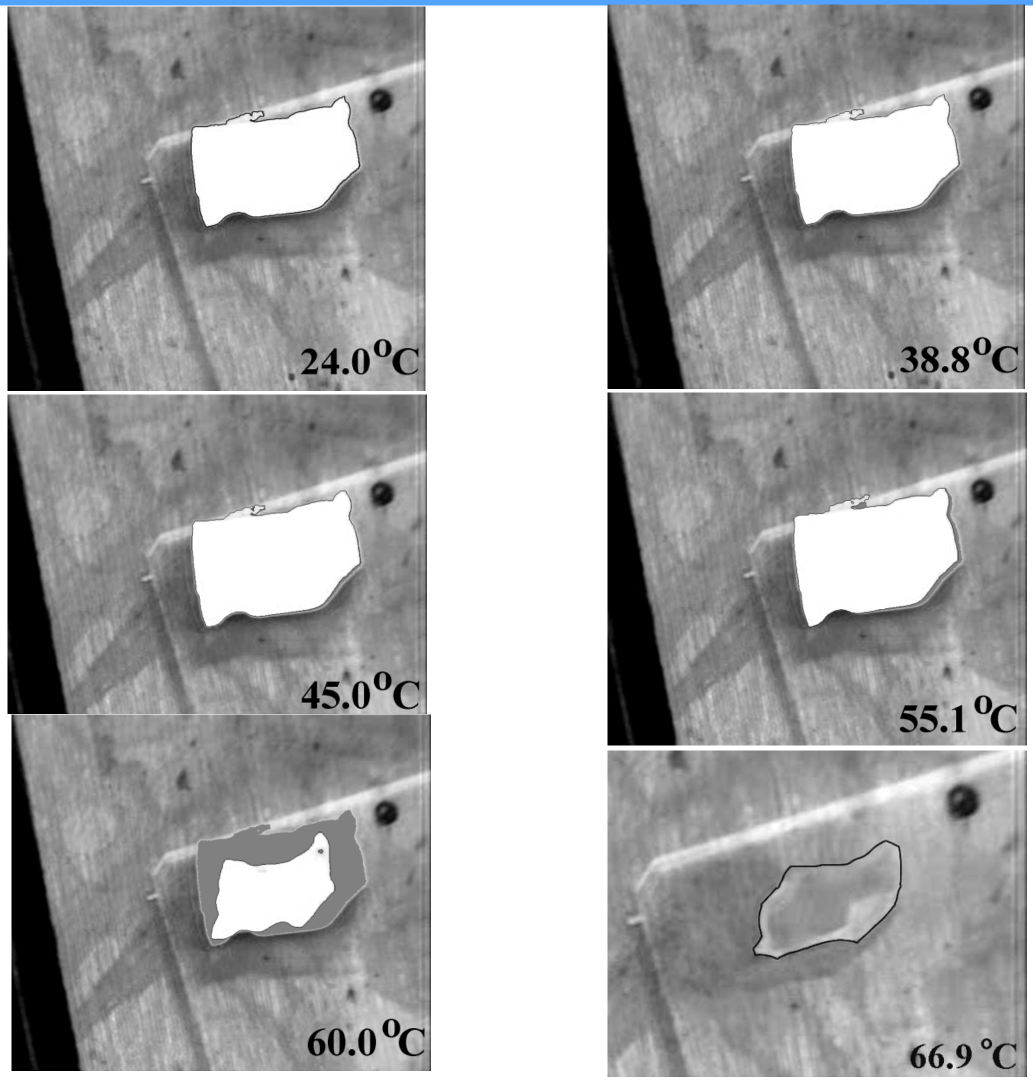

R. Srikar, T. Gambaryan-Roisman, C. Steffes, P. Stephan, C. Tropea, A.L. Yarin. Int. J. Heat and Mass Transfer v. 52, 5814-5826 (2009).

Drop/Spray Cooling through Nanofiber Mats: PAN Does Not Shrink Even at 250 C

Mechanical & Industrial Engineering

Temperature Field

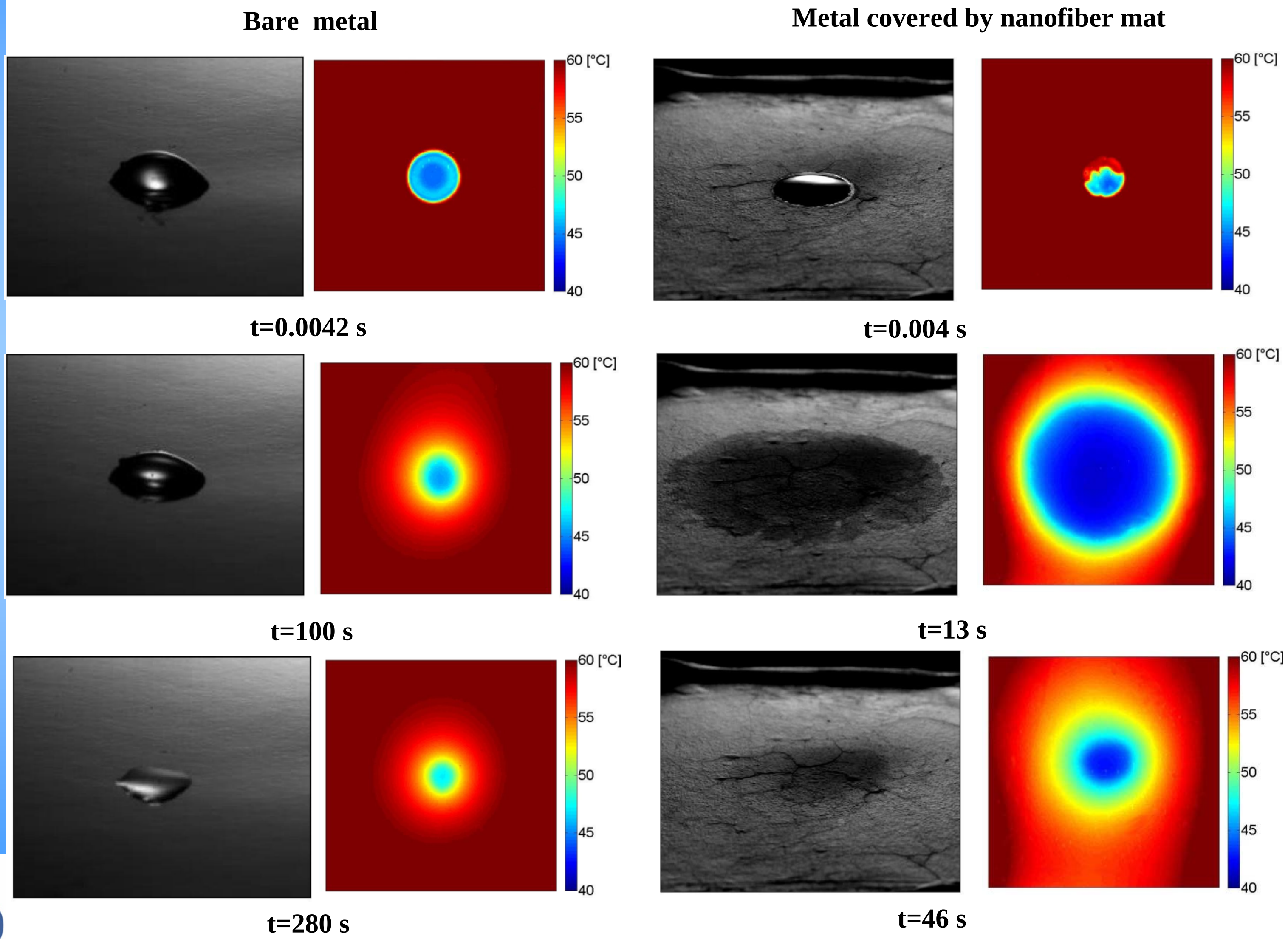

Mechanical & Industrial Engineering

Drop/Spray Cooling through Nanofiber Mats

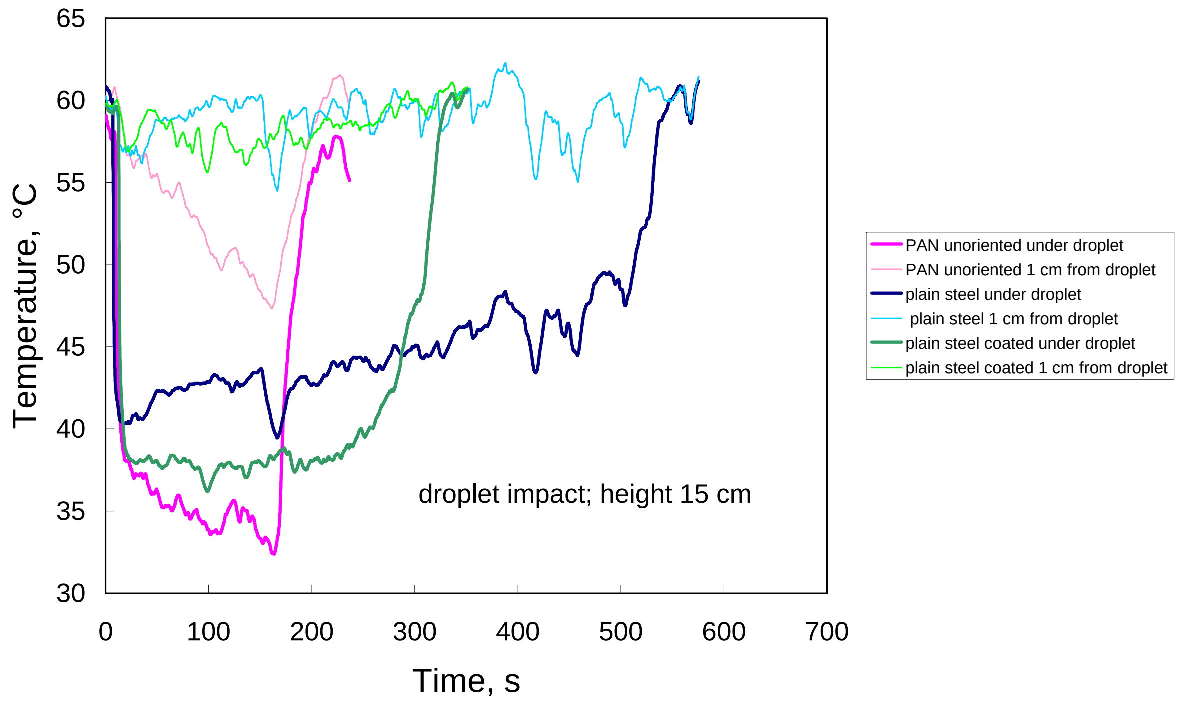

An attractive way for cooling high-heat flux components in microelectronics (e.g. on board of UAVs), as well as server rooms

Mechanical & Industrial Engineering

Bare Surface: The Leidenfrost Effect

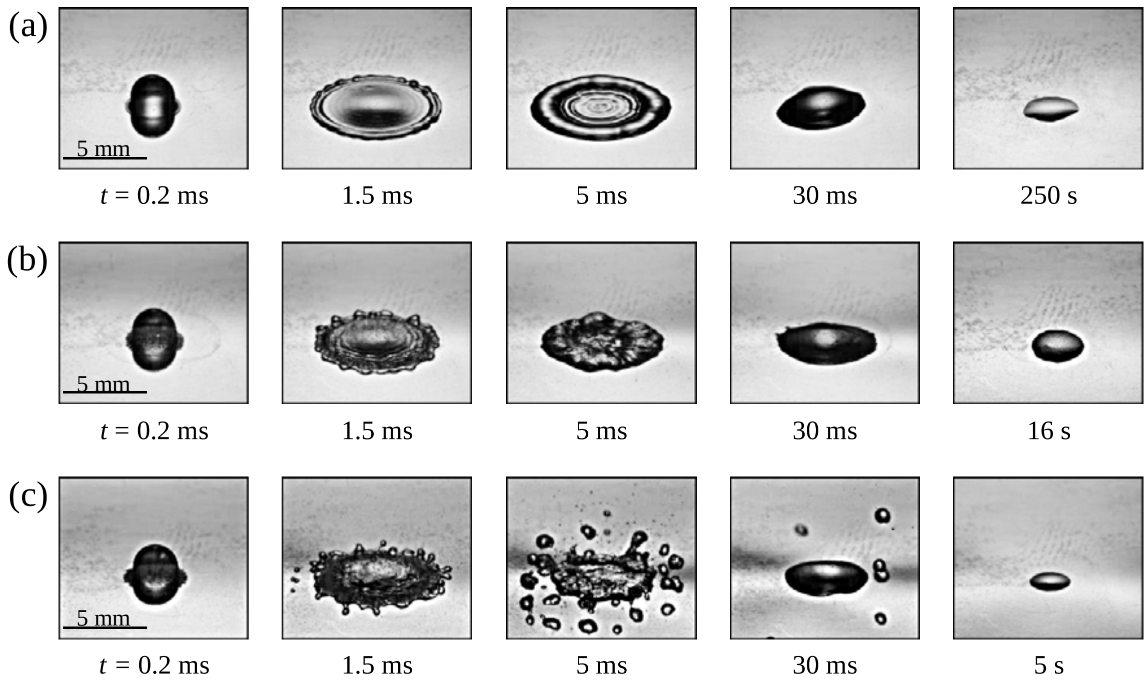

(a) 60°C, (b) 220°C, and (c) 300°C

Mechanical & Industrial Engineering

Nano-Textured Surface: The Anti-Leidenfrost Effect

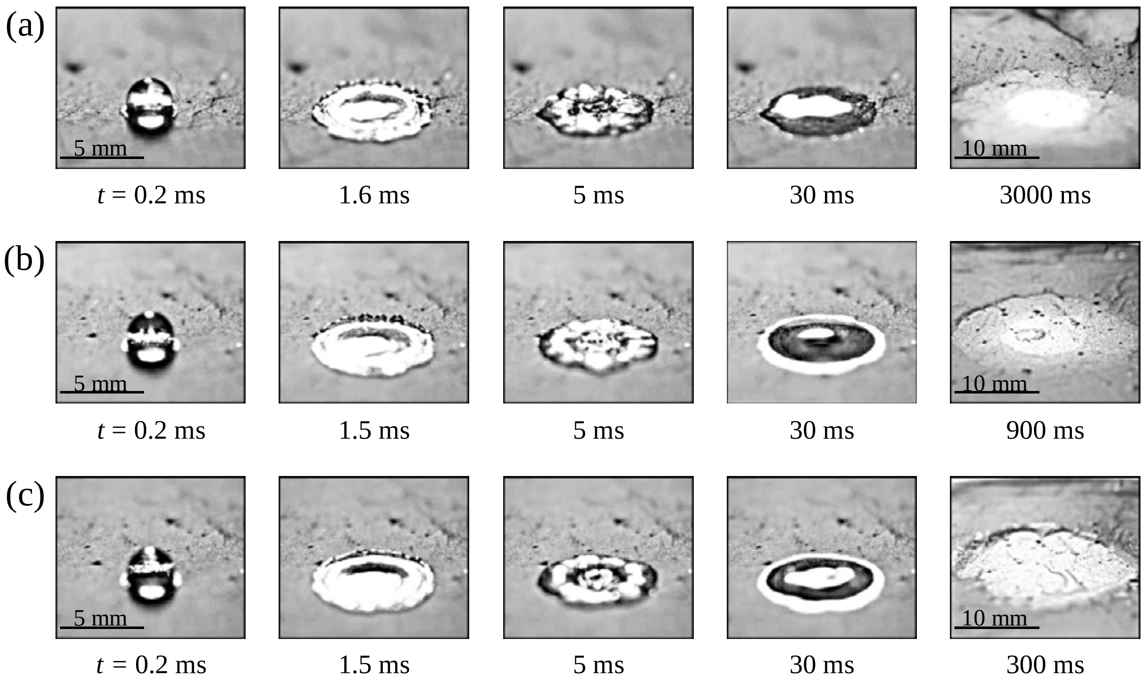

(a) 60°C, (b) 220°C, and (c) 300°C

Australian Thorny Devil Lizard

Mechanical & Industrial Engineering

Thorny Devil Copper Nanofibers

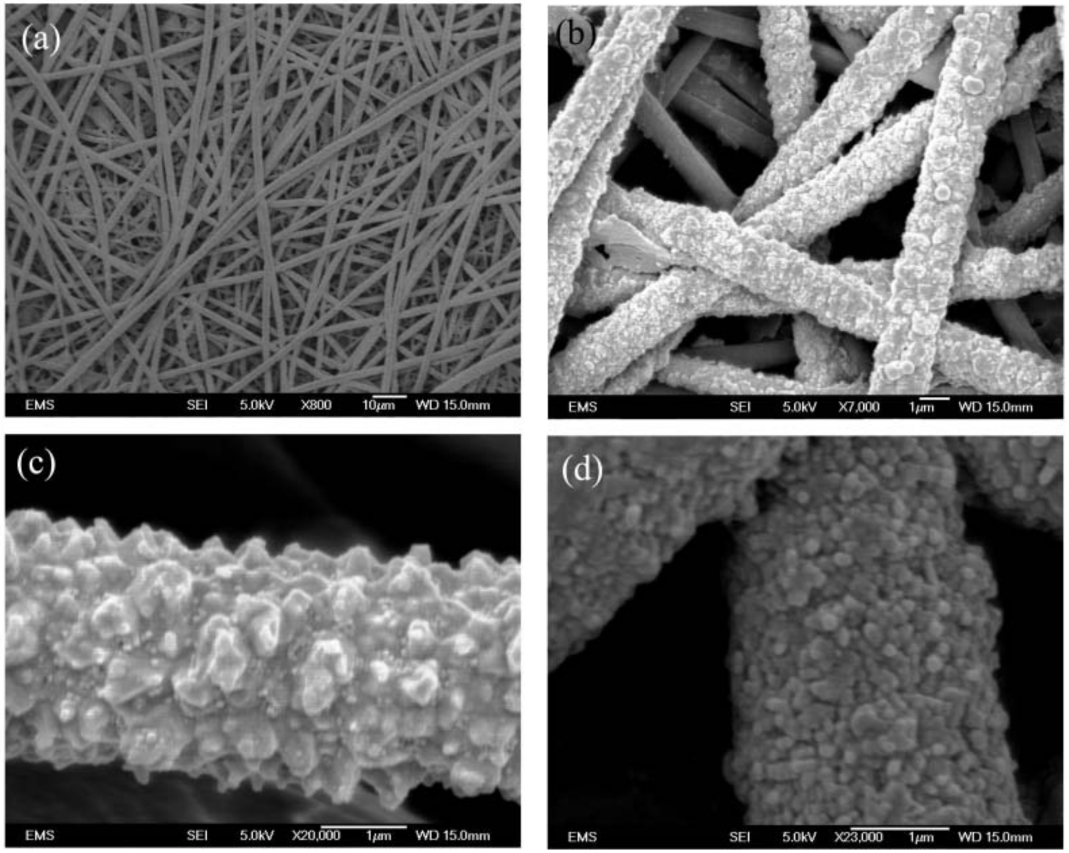

Thorny Devil Nanofibers: Fractal Surfaces?

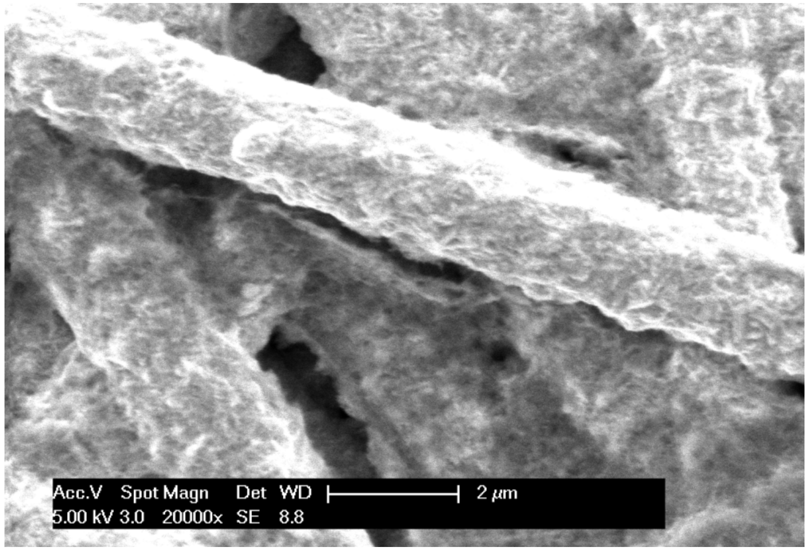

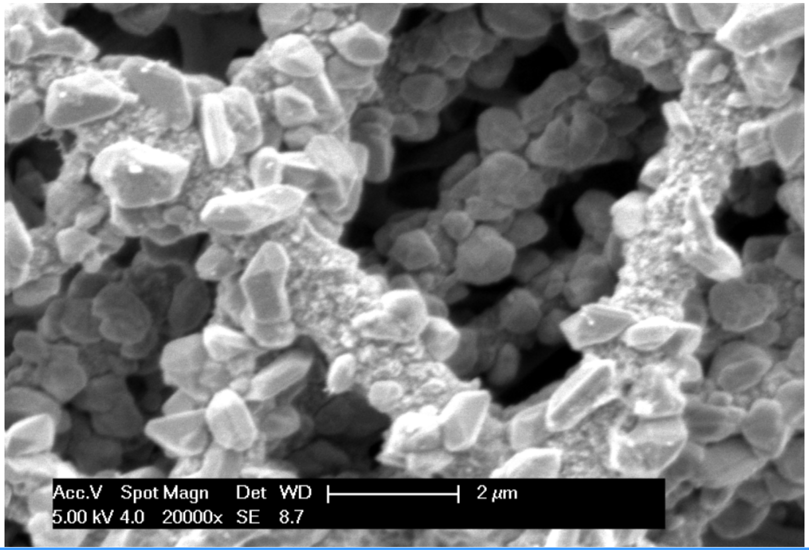

Mechanical & Industrial Engineering

Silver Nanofibers: Dendrite-Like

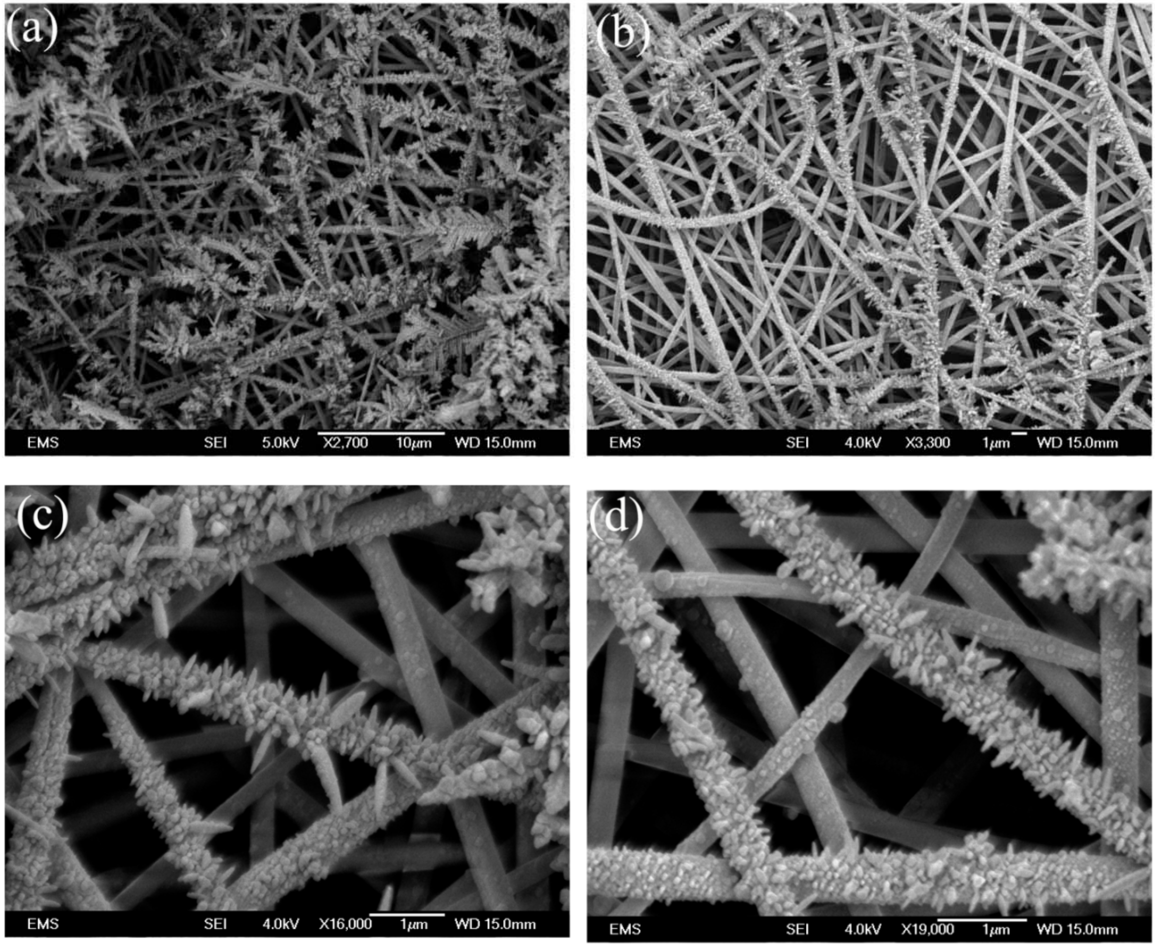

Nickel Nanofibers: Rough and Smooth Domains

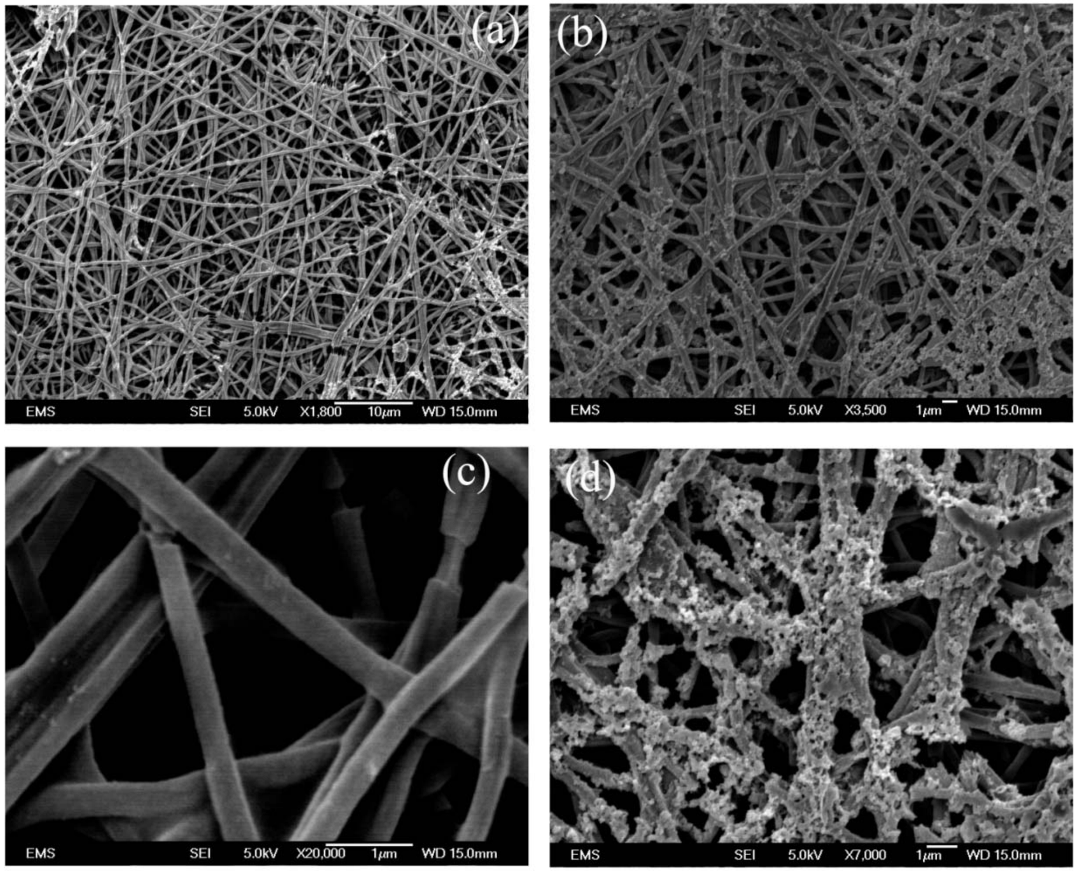

Gold Nanofibers: Rather Smooth

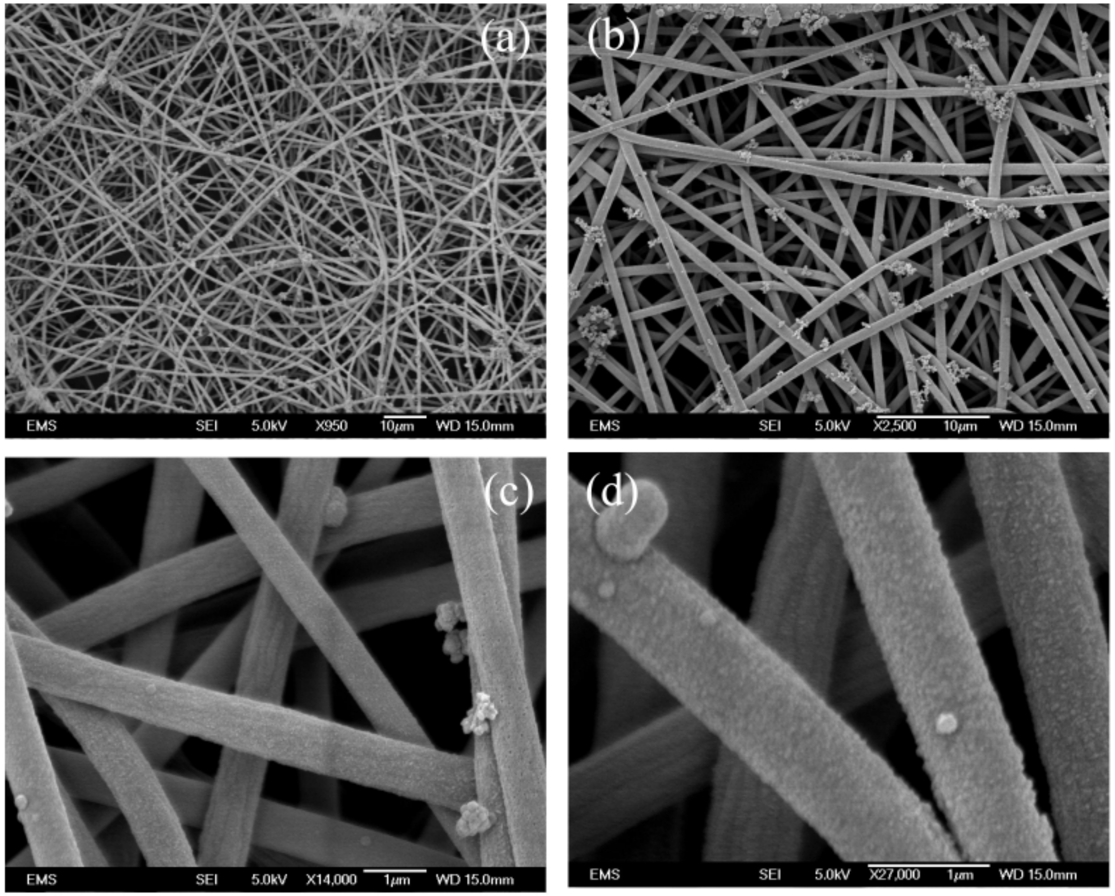

Mechanical & Industrial Engineering

Experimental Setup

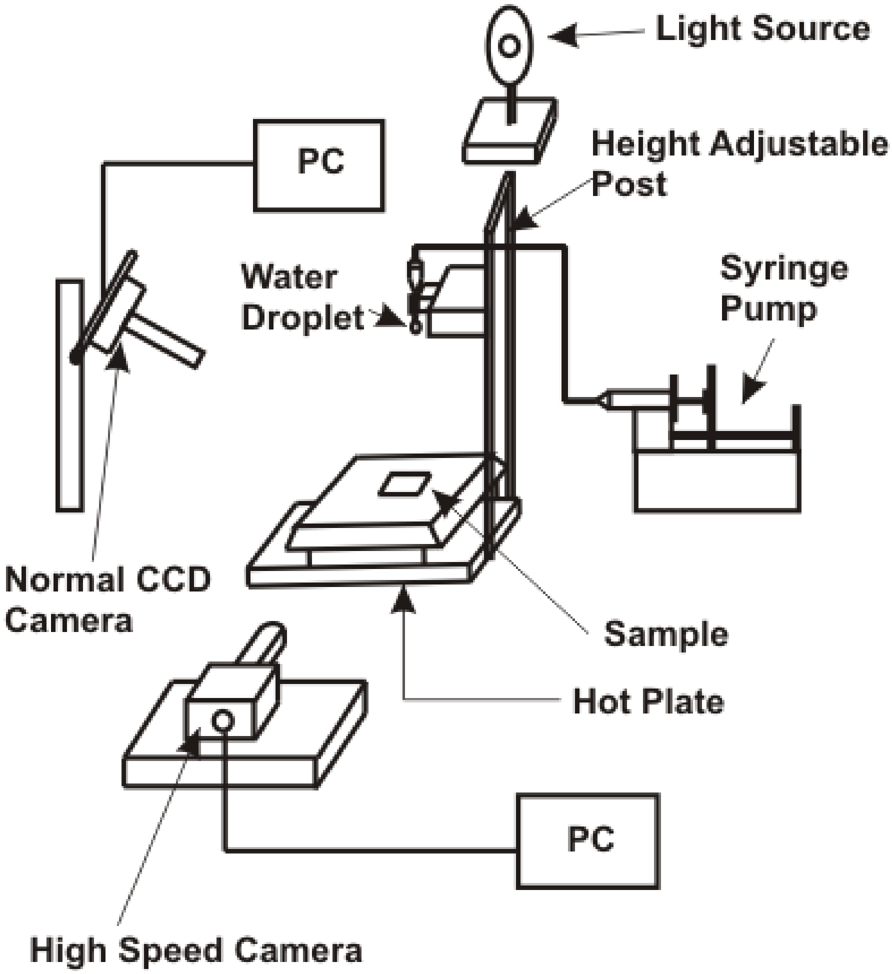

Mechanical & Industrial Engineering

Drop Impact from Height of 3.55 cm at Copper Thorny Devil Nanofibers at 150 C

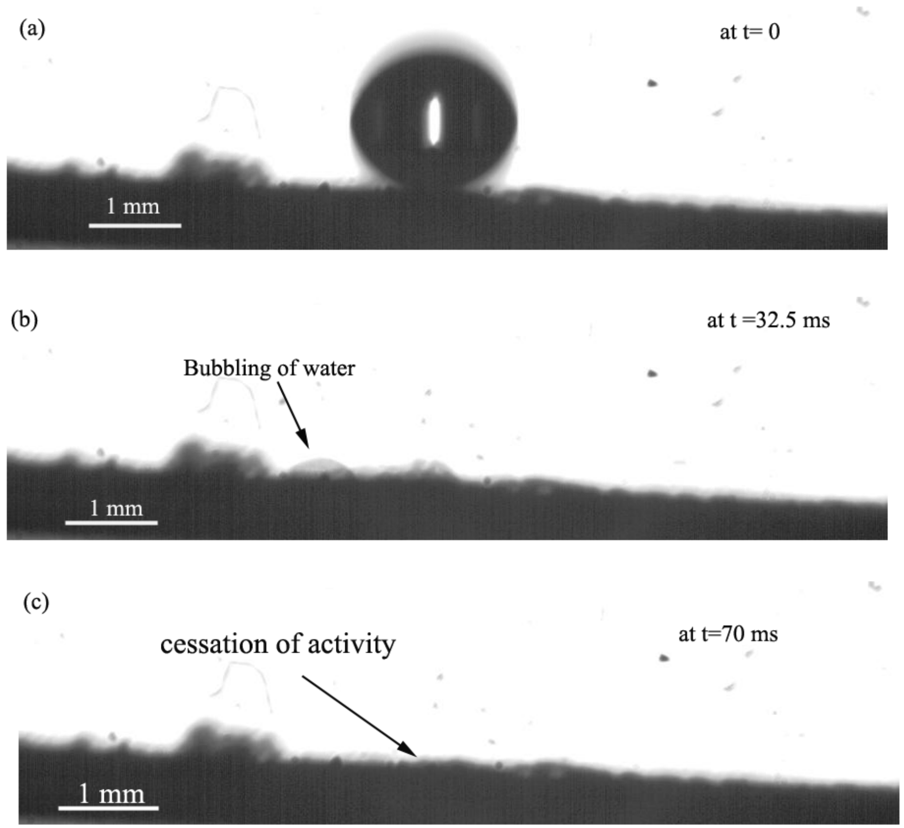

Mechanical & Industrial Engineering

The Anti-Leidenfrost Effect on Copper Thorny Devil Nanofibers at 172.2 C

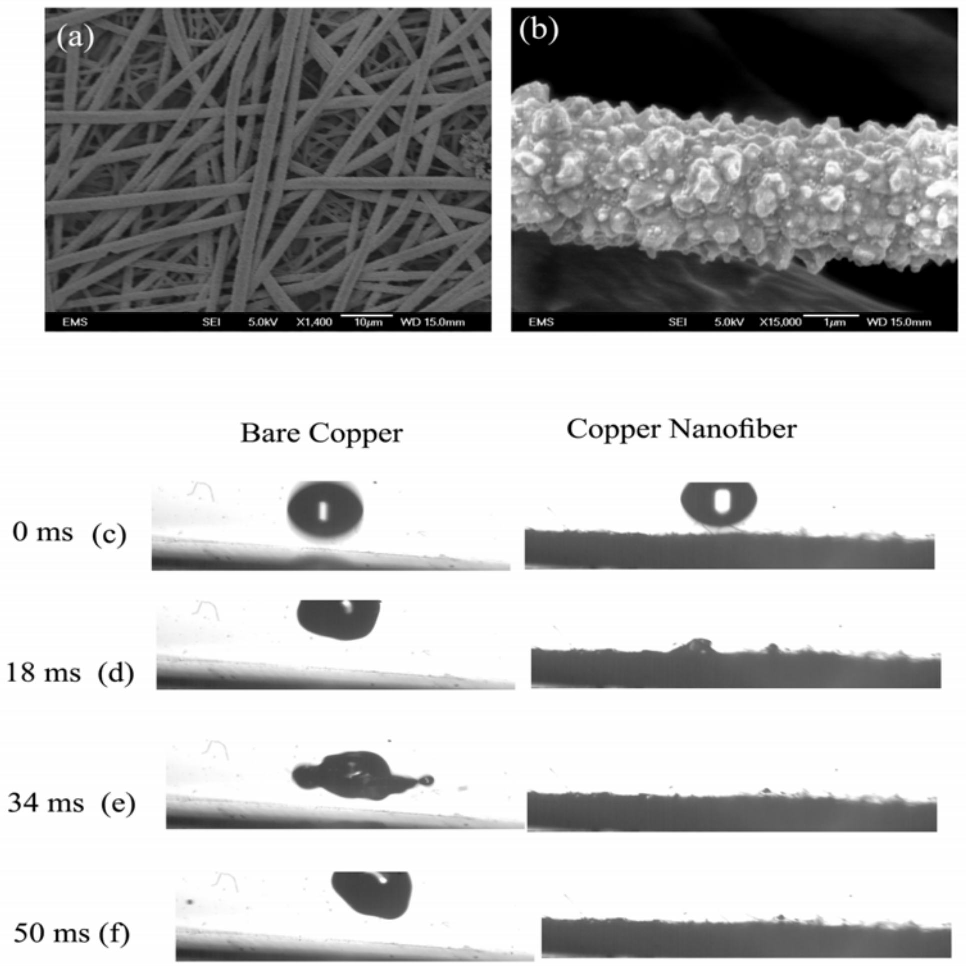

Drop Impact at Thorny Devil Nanofibers at 125 C

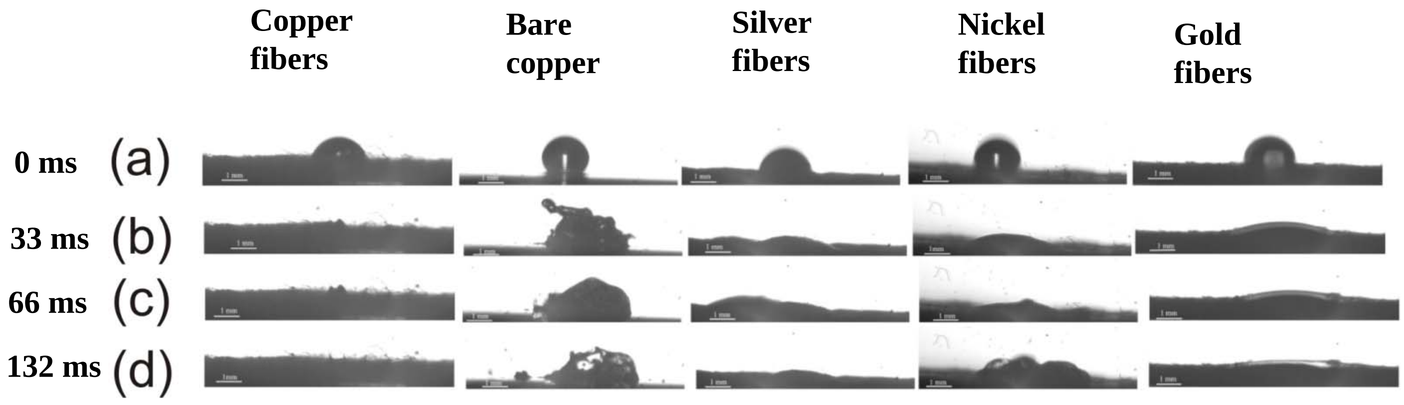

Thermal diffusivities:
Cu-1.12; Ag-1.66; Ni-0.155; Au-1.27 (sq.cm/s);
Water evaporation on copper and silver fibers is the fastests but on gold-the slowest! Thorny devils win!

Drop Impact at Thorny Devil Nanofibers at 150 C

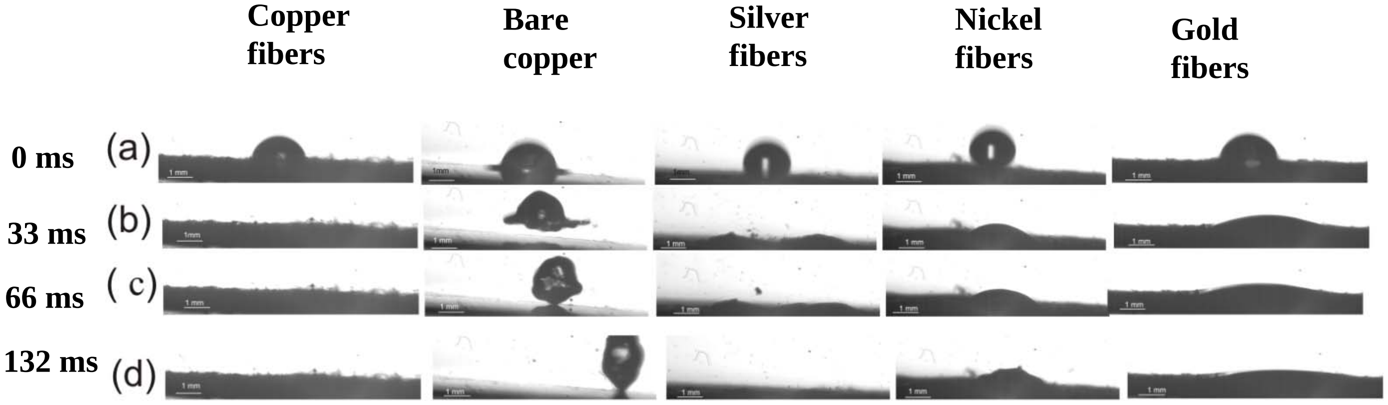

Drop Impact at Thorny Devil Nanofibers at 200 C

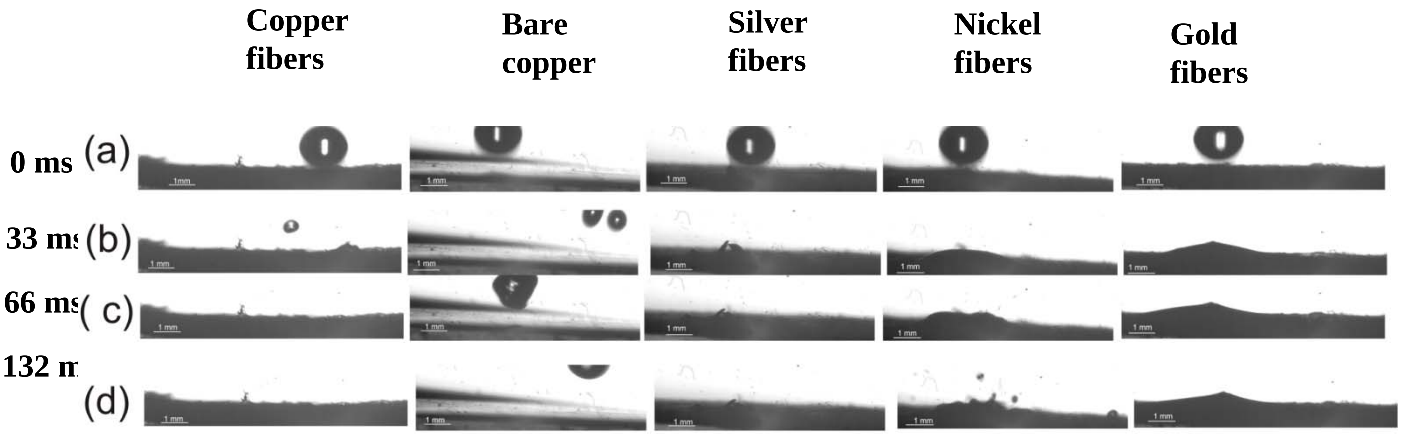

Mechanical & Industrial Engineering

Mass Losses due to “Atomization” during Evaporative Cooling Through Copper Nanofibers

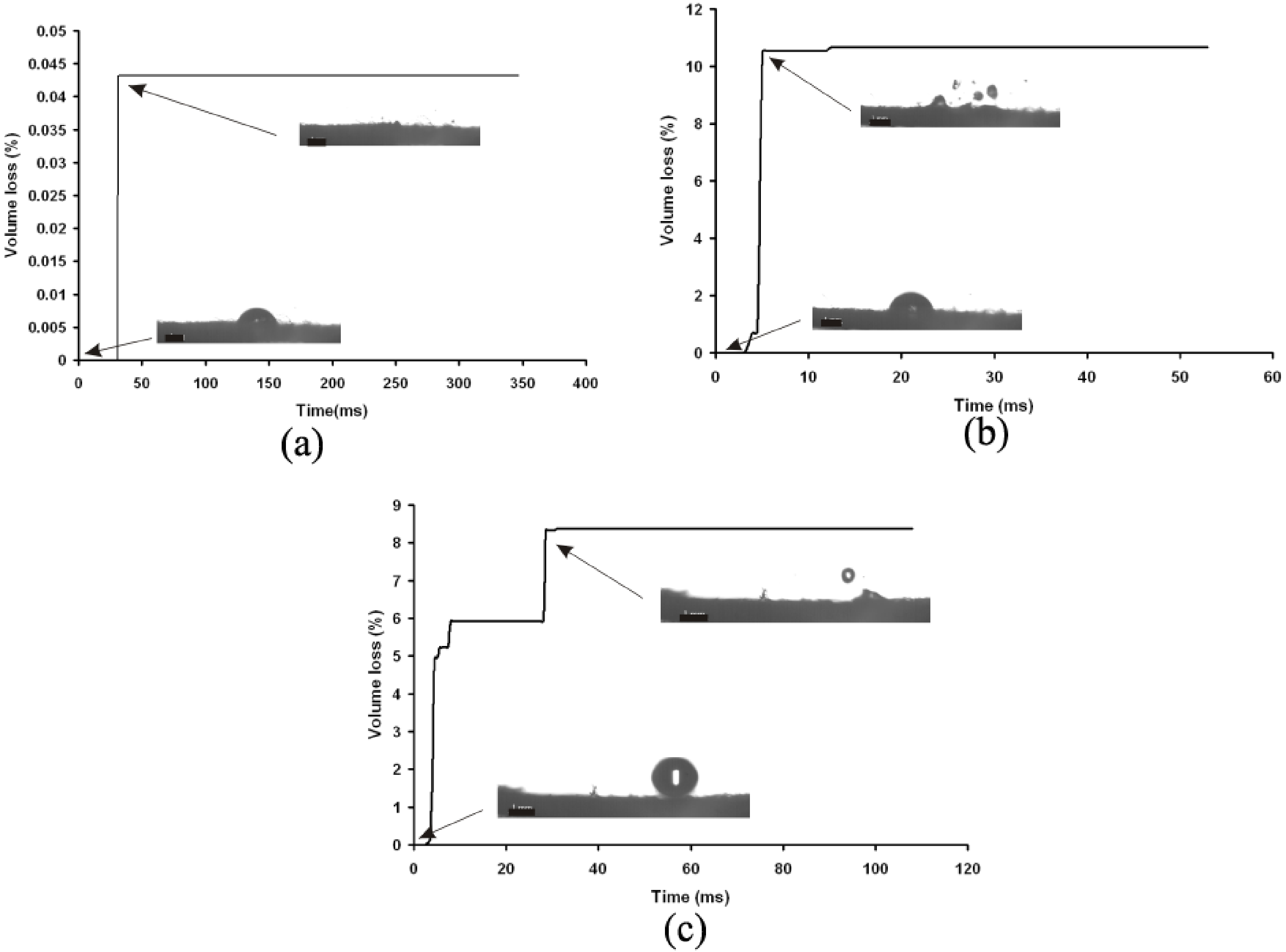

Copper fibers:
a-125 C,
b-150 C,
c-200 C

Mechanical & Industrial Engineering

Mass Losses due to "Atomization" during Evaporative Cooling on Bare Copper

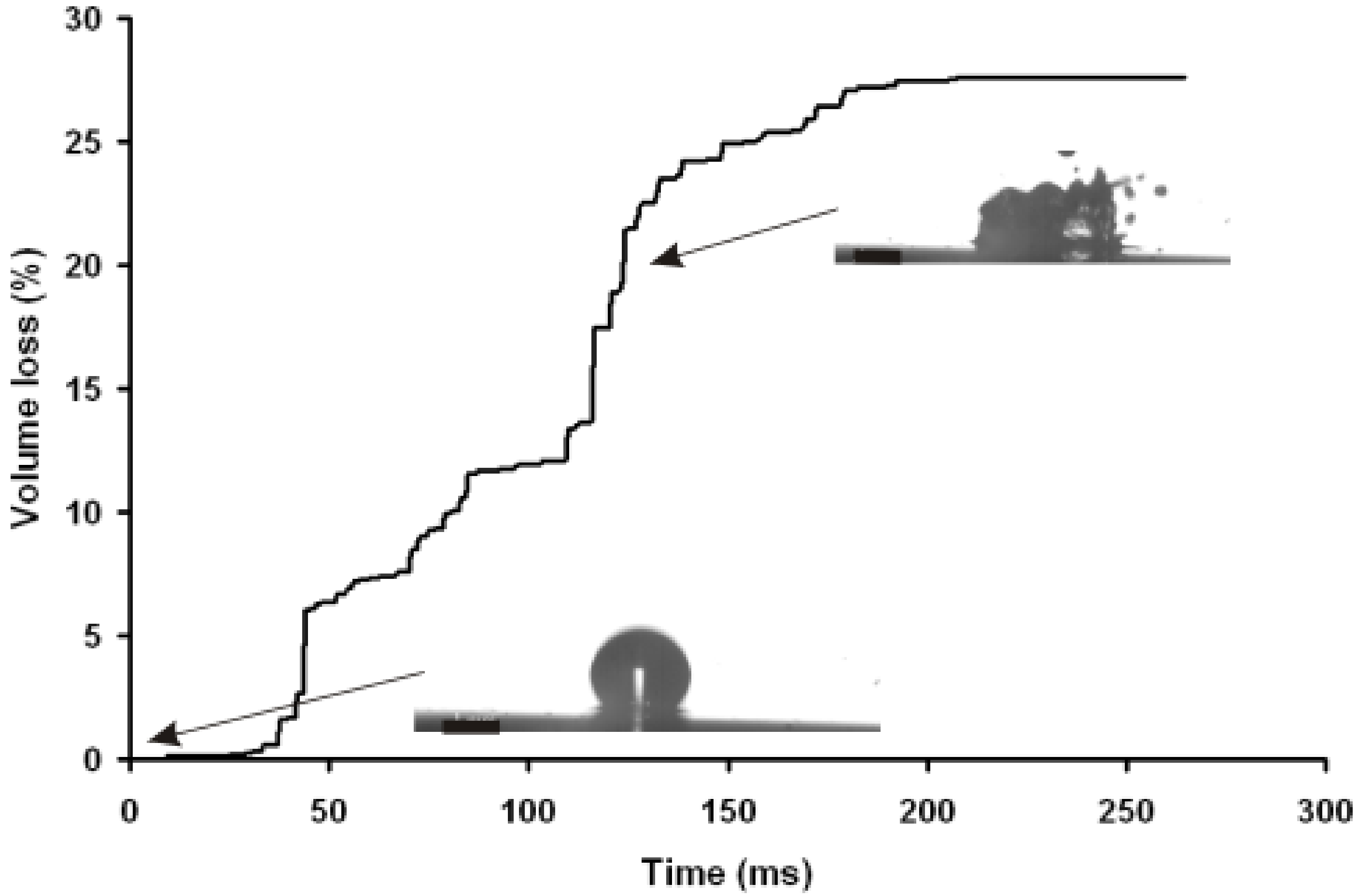

Bare copper

Mass Losses due to "Atomization" during Evaporative Cooling on Silver Nanofibers

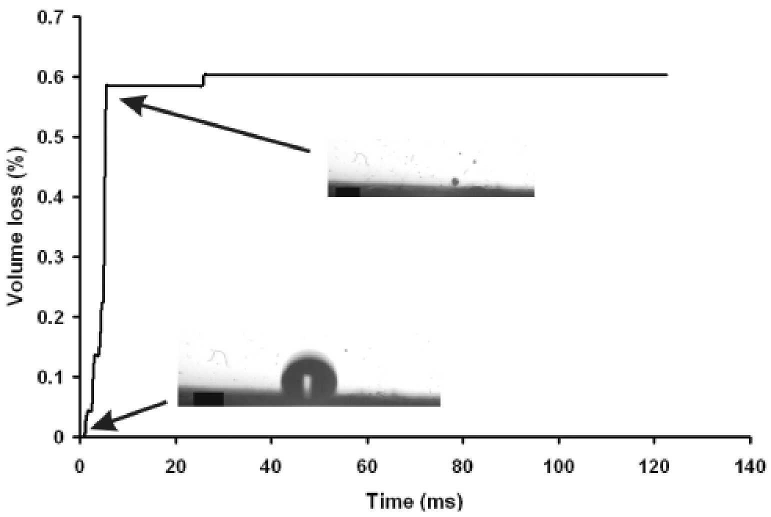

(a)

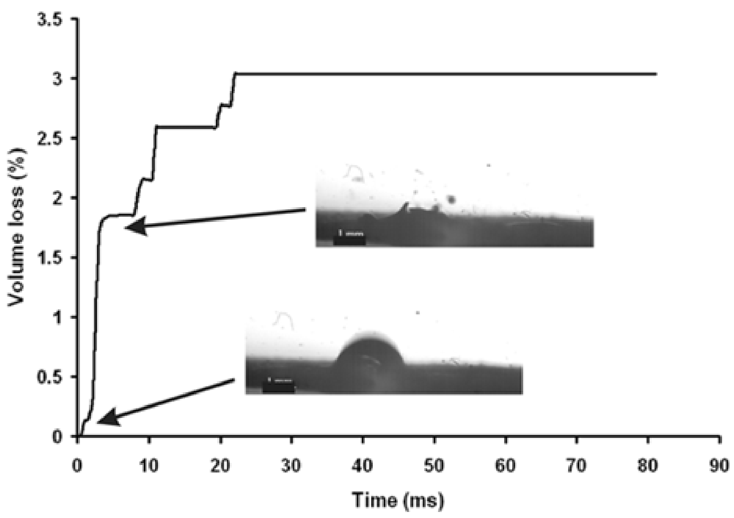

(b)

Silver fibers:
a- 150 C
b- 200 C

Mass Losses due to "Atomization" during Evaporative Cooling on Nickel Nanofibers

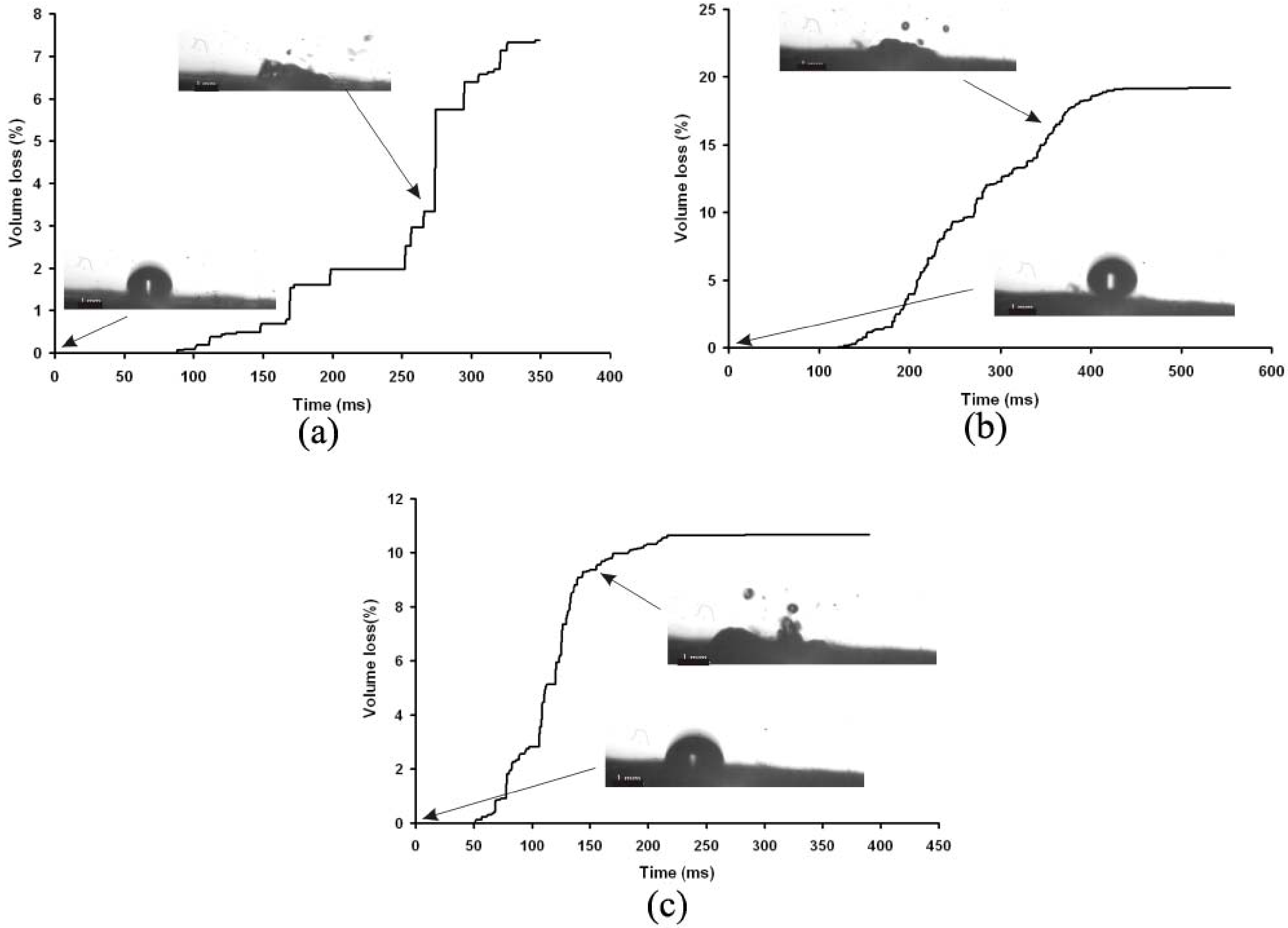

Silver fibers:
a- 125 C
b- 150 C
c- 200 C

Mechanical & Indus
Engineeri

The Resulting Spreading Factor and Cooling Rate for Copper Nanofibers at Different Impact Speeds

h (cm)	V (cm/s)	Δt (ms)	ξ	p	J-evap. (kW/cm^2)
3.55	83.46	70	2.6	0	**0.607**
6.15	109.85	58	2.85	0	**0.575**
8.75	131.02	53.5	3.02	0	**0.555**
11.15	147.91	52.5	3.15	0	**0.521**
13.75	164.25	47	3.41	0	**0.543**

The Resulting Spreading Factor and Cooling Rate for Metal-Plated Nanofibers at Different Impact Speeds and the the Non-Zero "Atomization" Ratio p

Material	Temperature (^0C)	Δt (ms)	p	J-evap. (kW/ cm^2)
Bare copper	125	264	0.32	0.256
	150	N/A	N/A	N/A
	200	N/A	N/A	N/A
Copper nanofibers	125	172.5	0.09	0.136
	150	53	0.16	**0.392**
	200	52	0.13	**0.408**
Silver nanofibers	125	170	0.05	**0.138**
	150	128.5	0.056	**0.181**
	200	55.5	0.08	**0.407**
Nickel nanofibers	125	355	0.124	0.061
	150	600	0.25	0.031
	200	388	0.15	0.054
Gold nanofiber	125	495	0.05	0.047
	150	633.5	0.05	0.037
	200	468	0.05	0.049

Mechanical & Industrial Engineering

Co-electrospinning: Compound Nanofibers and Nanotubes

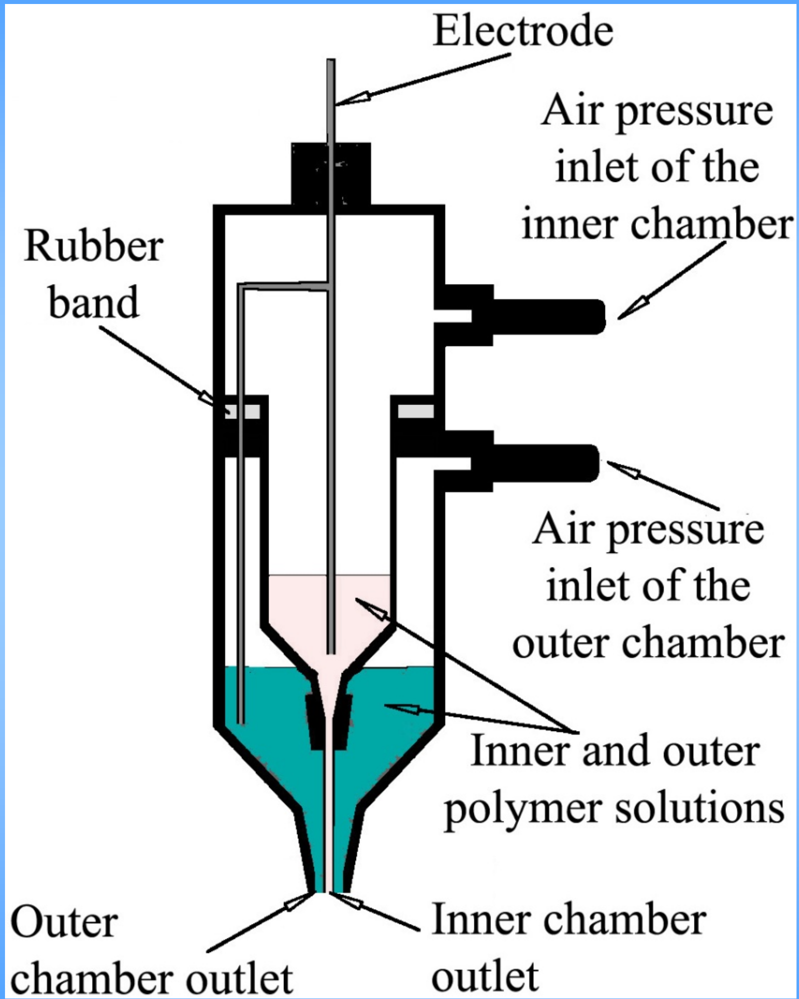

Solution: PEO (1e6) 1% in ethanol/water

Inner solution contains 2% bromophenol
Outer solution contains 0.2% bromophenol

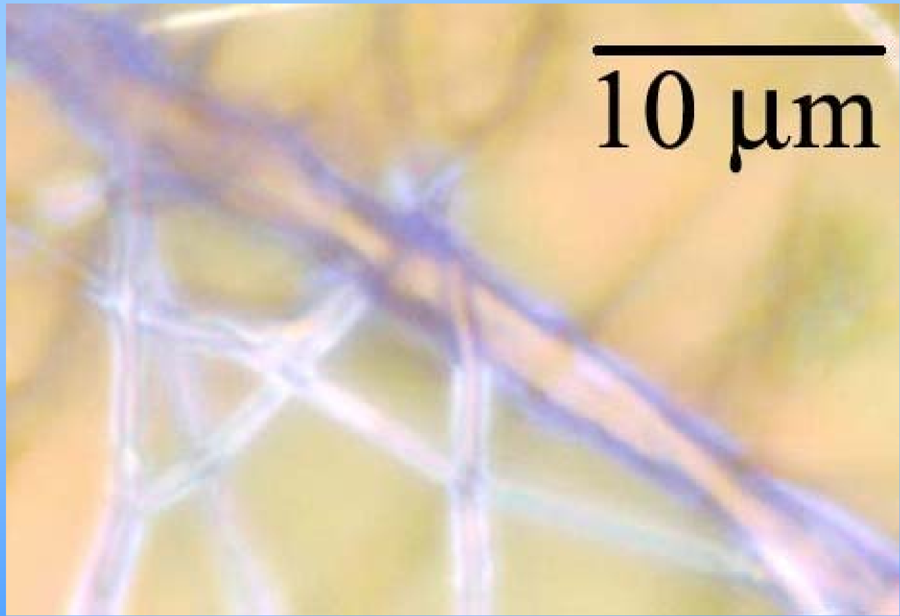

Mechanical & Industrial Engineering

Sun Z, Zussman E, Yarin A L, Wendorff J H, Greiner A, *Advanced Materials* 15, 2003

Co-electrospinning

Core: PMMA

Shell: PAN

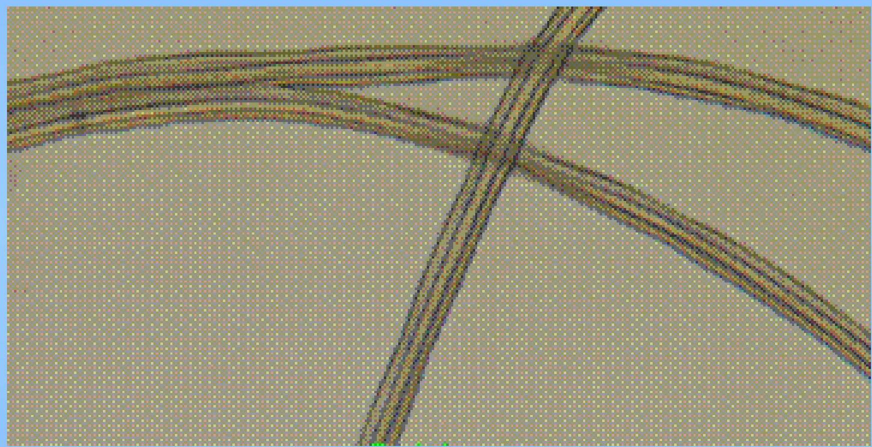

Zussman E, Yarin A L, Bazilevsky A.V., R. Avrahami, M. Feldman, *Advanced Materials* 18, 2006

Self-assembly: Nanoropes and Crossbars. A Sharpened Wheel – Electrsostatic Lens

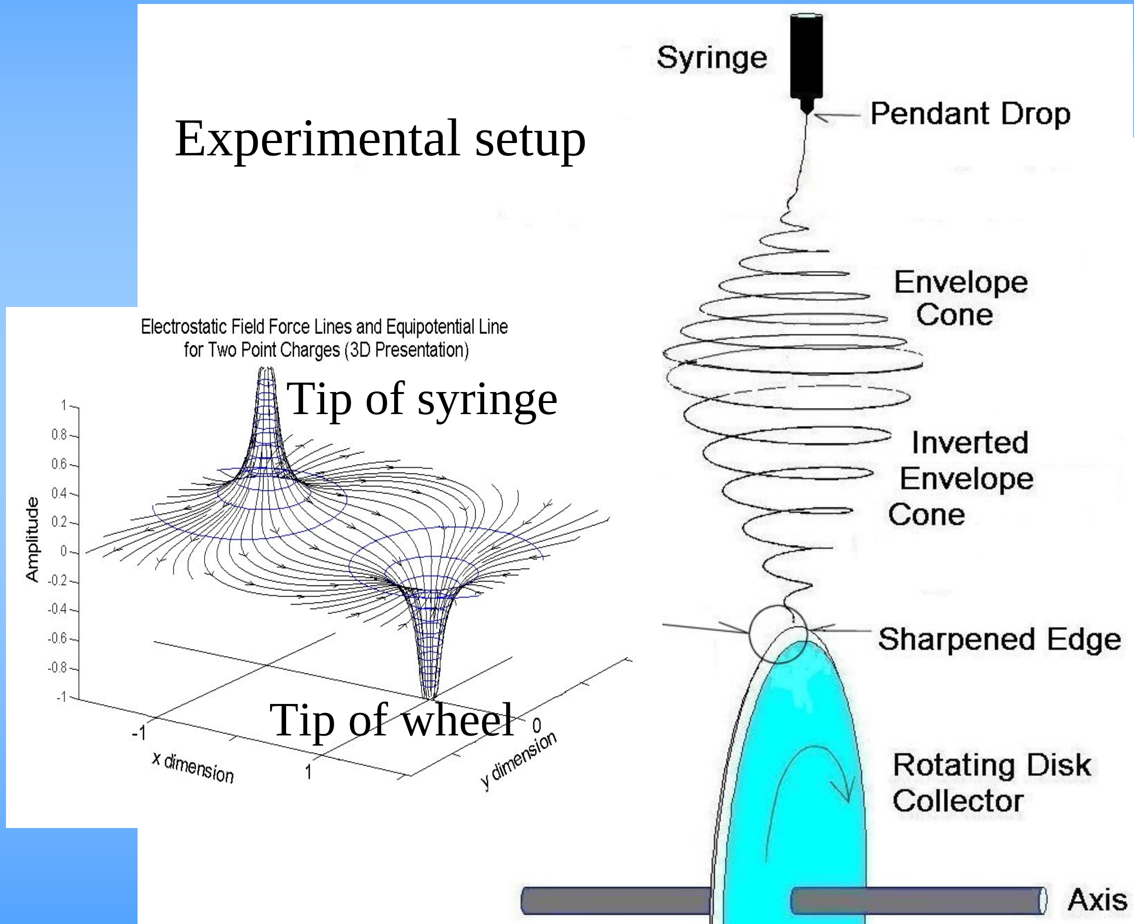

Plot of the electric field strength in the region of the wheel

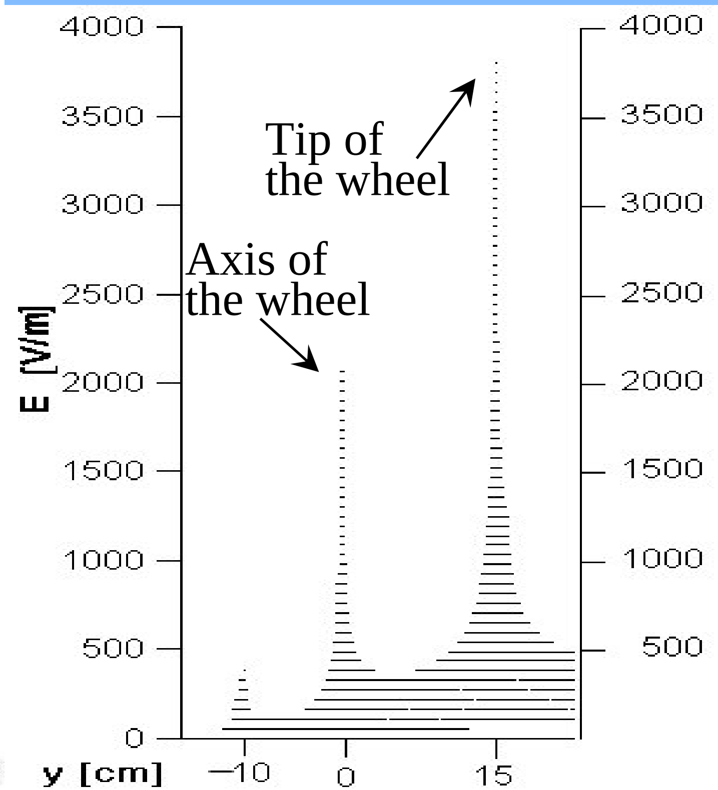

Mechanical & Industrial Engineering

Theron A, Zussman E, Yarin A L, *Nanotechnology* 12, 2001

Nanoropes

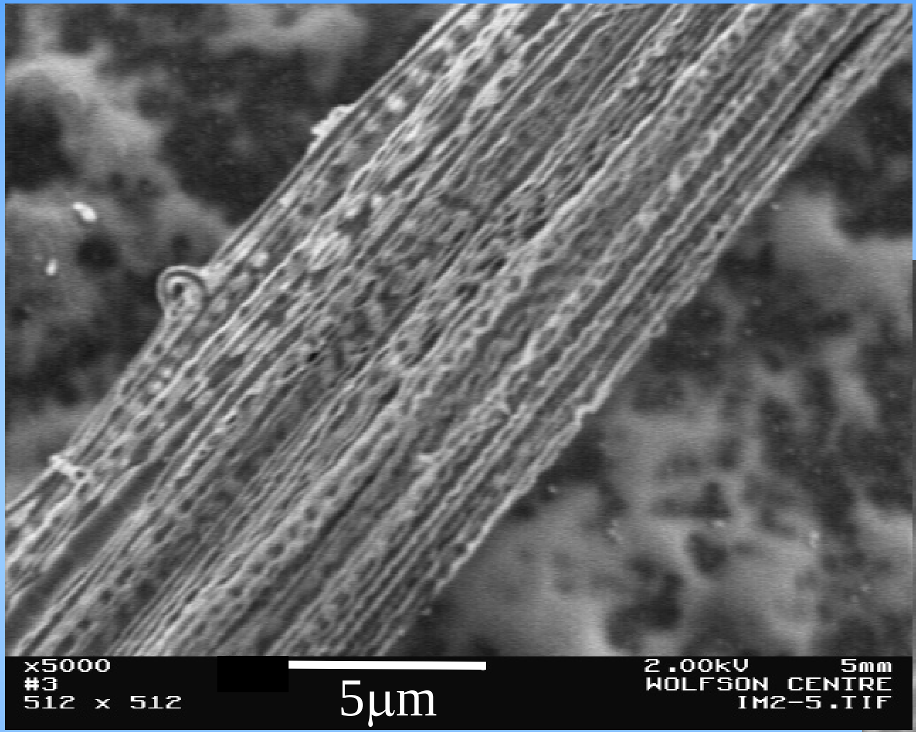

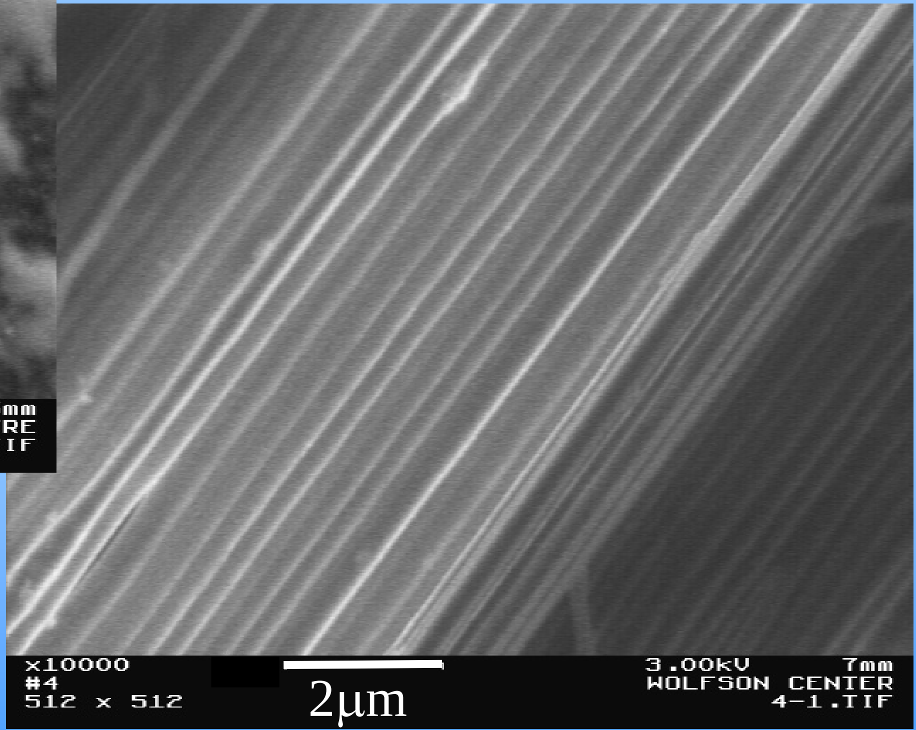

Mechanical & Industrial Engineering

Turbostratic Carbon Nanotubes

Core: PMMA

Shell: PAN

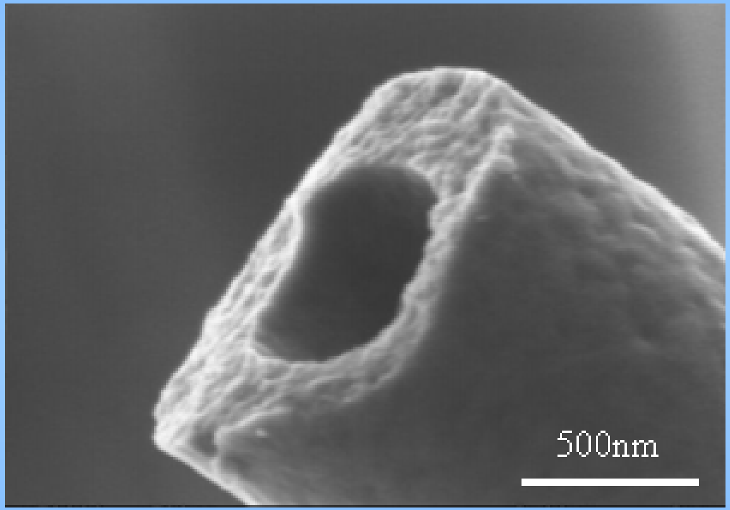

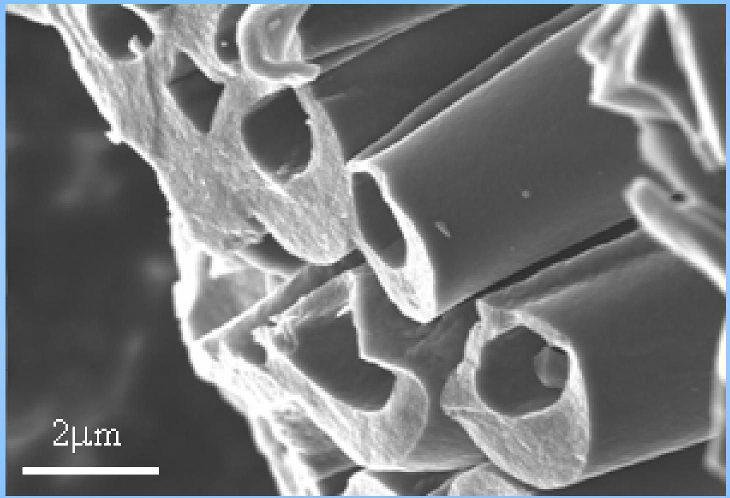

Mechanical & Industrial Engineering

Core-Shell Nanofibers from PMMA-PAN Emulsion

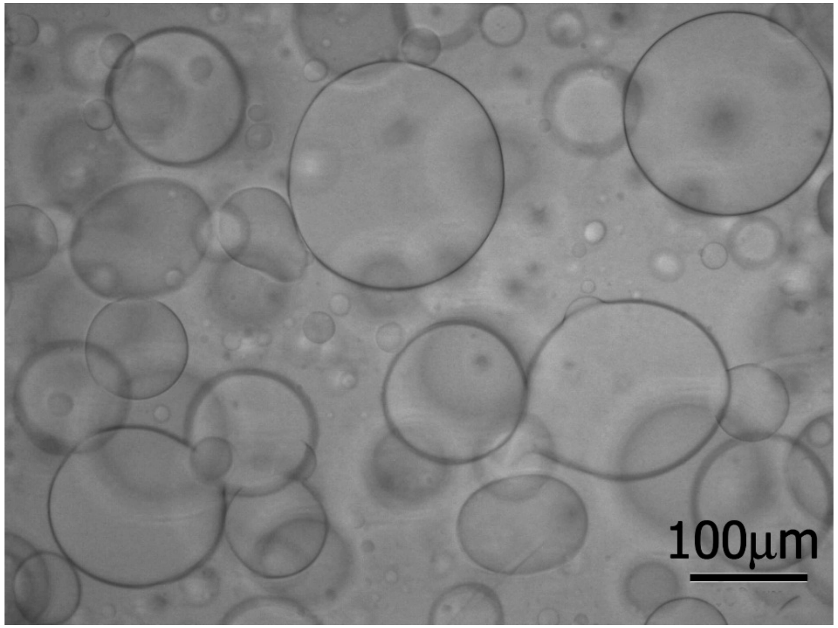

Optical appearance of a PMMA/PAN emulsion about 1 day after mixing of a homogeneous blend containing 6 wt% PMMA + 6% PAN in DMF

A.V.Bazilevsky, A.L. Yarin, C.M. Megaridis Langmuir v.23, 2311-2314 (2007).

Mechanical & Industrial Engineering

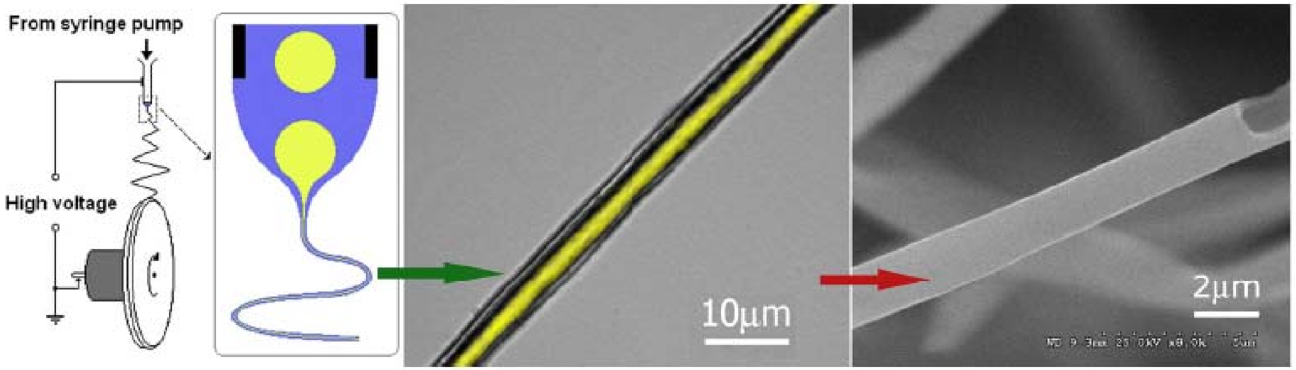

Experimental set-up and hollow carbon tubes

Pressure-driven Nanofluidics in Macroscopically Long Carbon Nanotubes

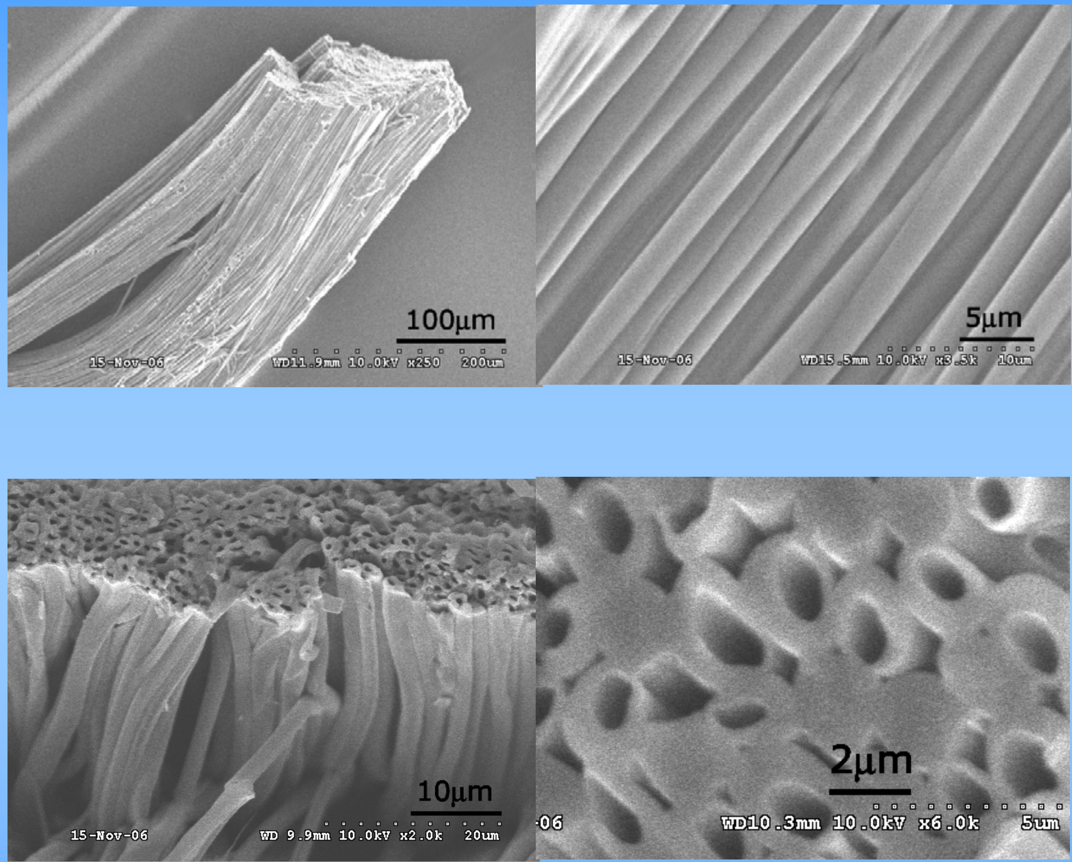

Bazilevsky AV, Yarin AL, Megaridis CM,
Lab on a Chip v. 7 152-160 (2008).

Mechanical & Industrial Engineering

Experimental Setup

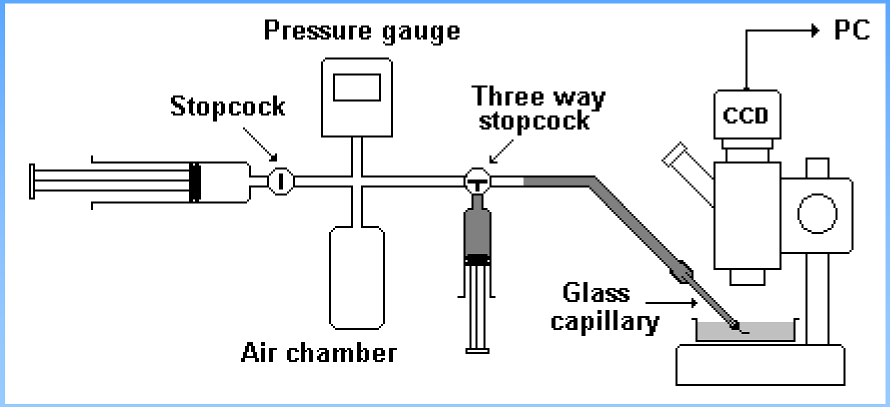

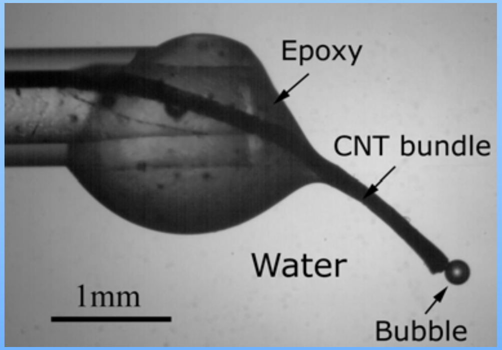

Mechanical & Industrial Engineering

Release Observation

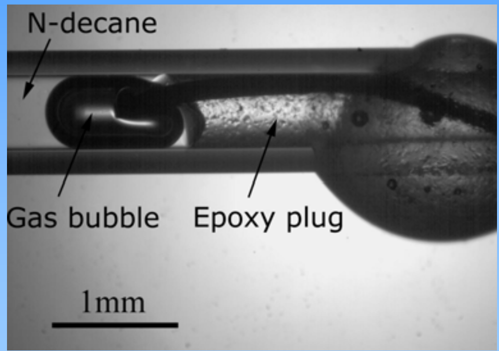

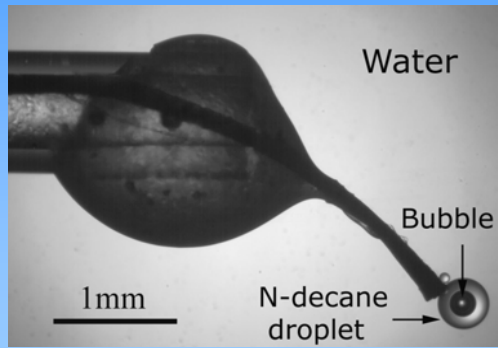

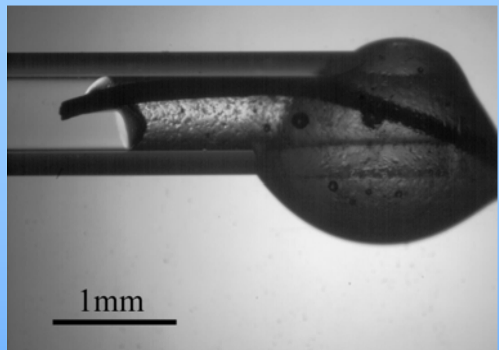

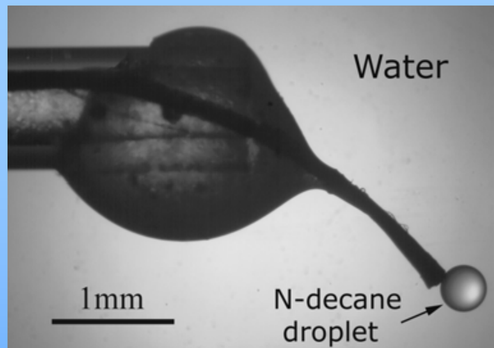

Mechanical & Industrial
Engineering

Air Flow Rate

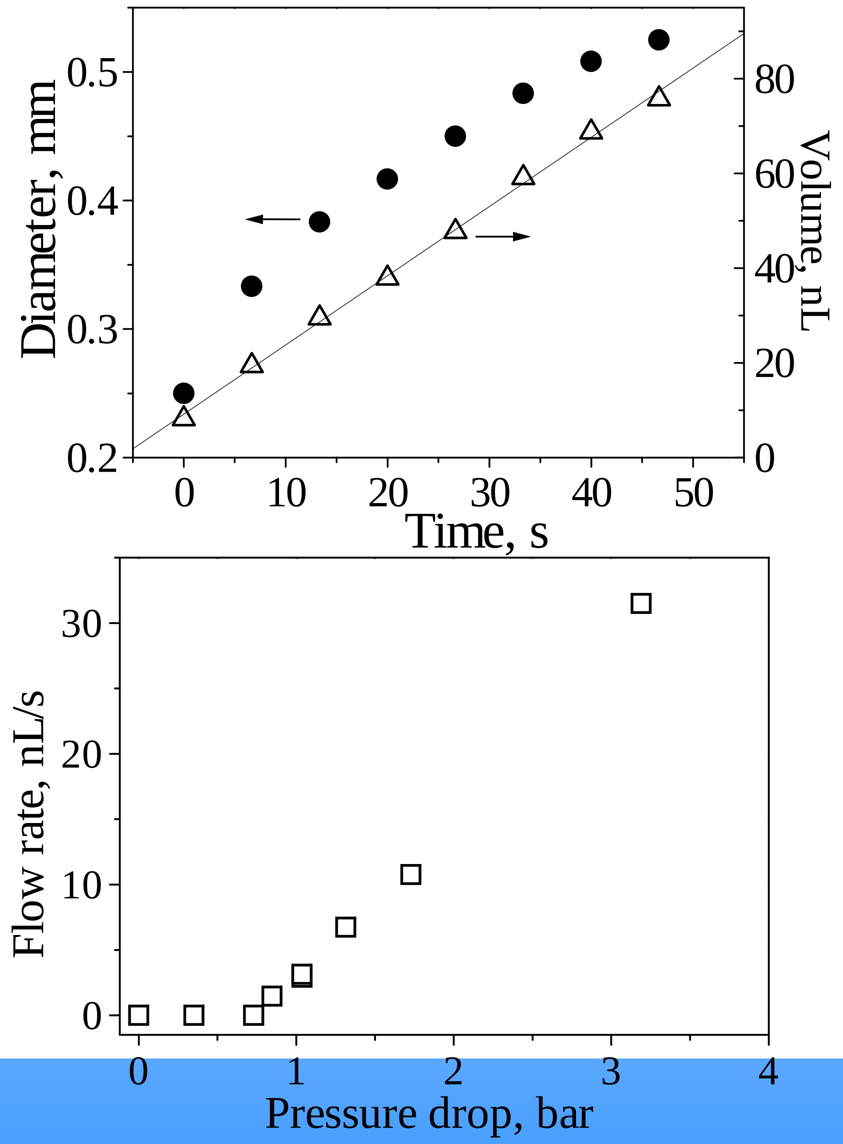

N-decane Flow Rate;
Recovering the Flow-carrying Inner Tube Diameter Distribution

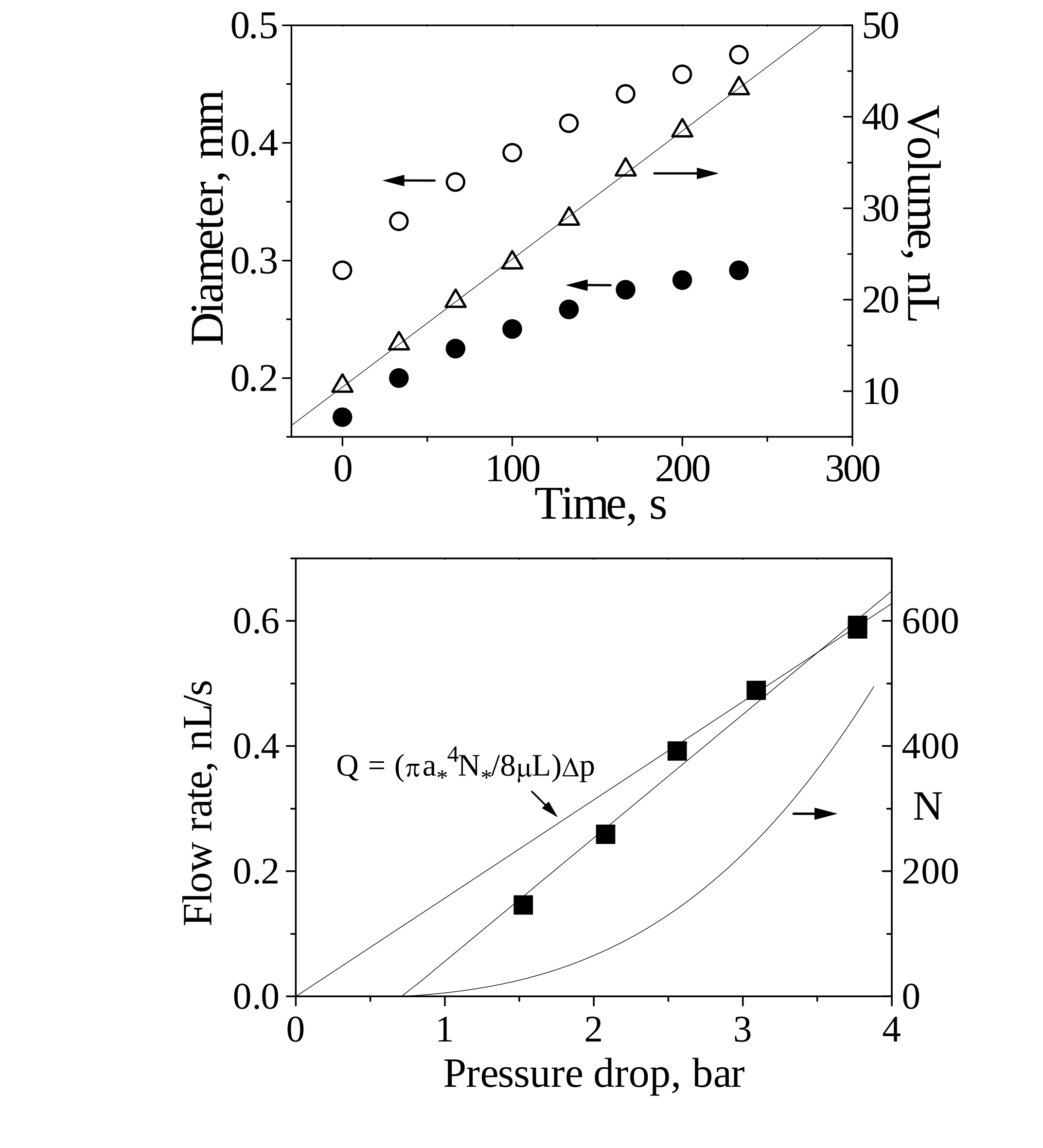

Mechanical & Industrial Engineering

Amendment to Poiseuille's Law

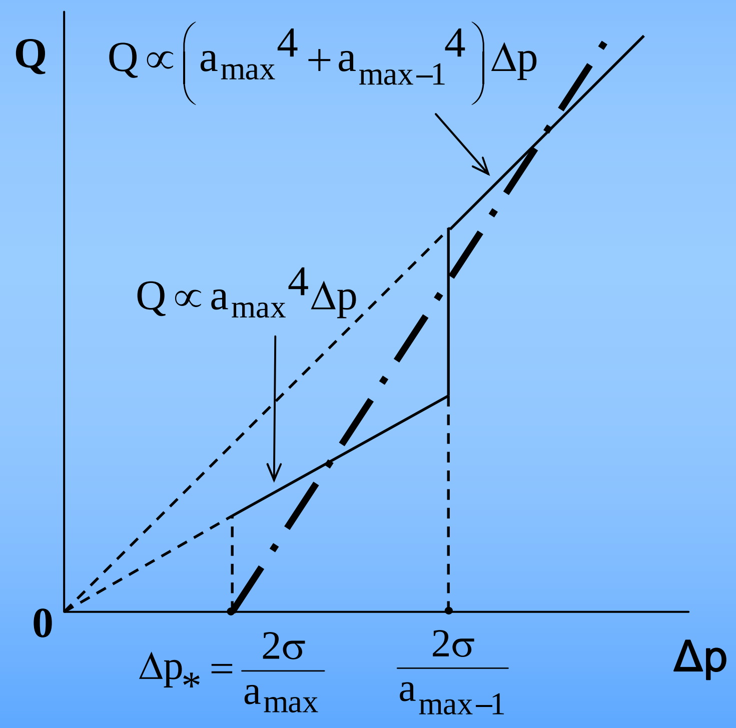

Mechanical & Industrial Engineering

Template Approach: Nanotube Strips

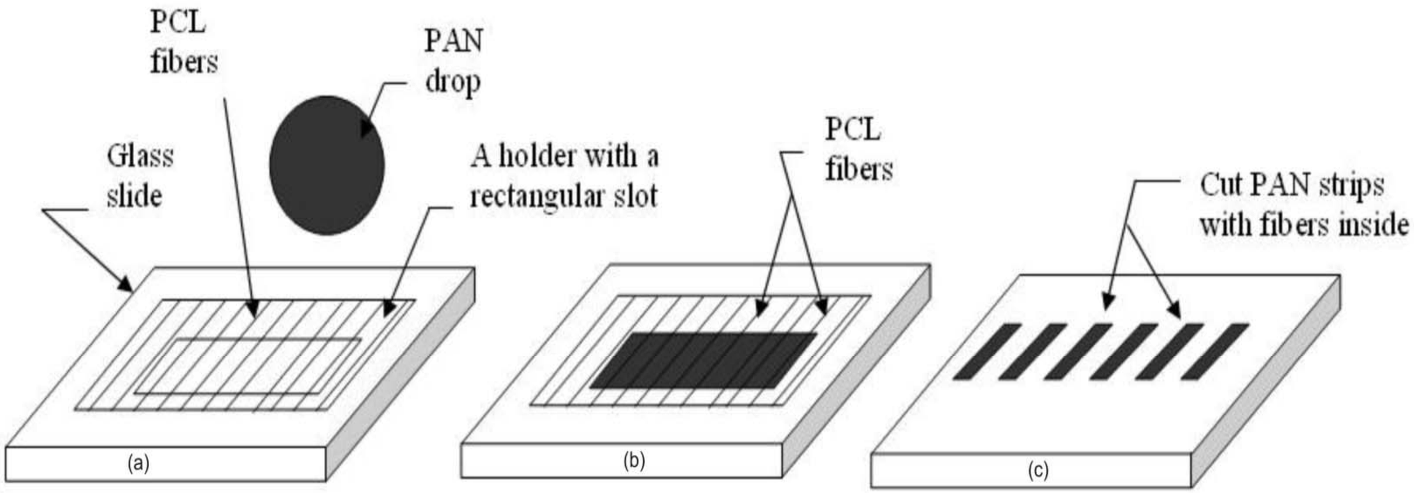

S.S. Ray, P. Chando, A.L. Yarin, Nanotechnology v. 20, 095711 (2009).

Entrapped Bubbles: Two-phase Flows

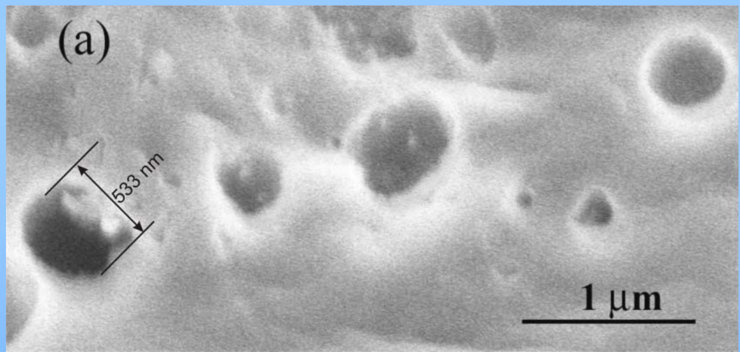

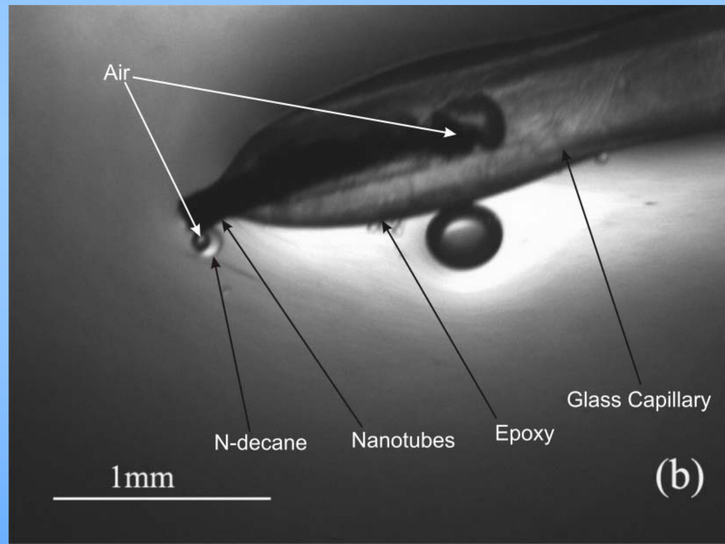

Mechanical & Industrial Engineering

Modeling of Entrapped Air in n-Decane

Four possible situations describing air-liquid flow

1

2

3

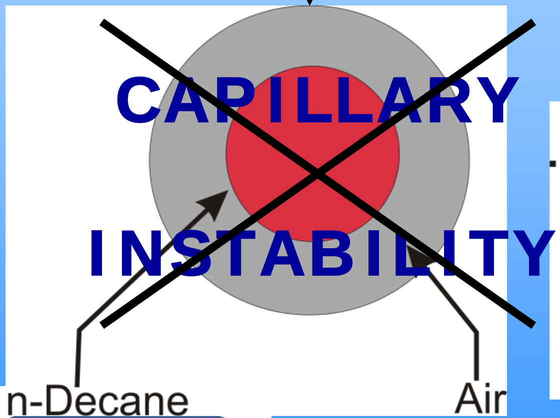

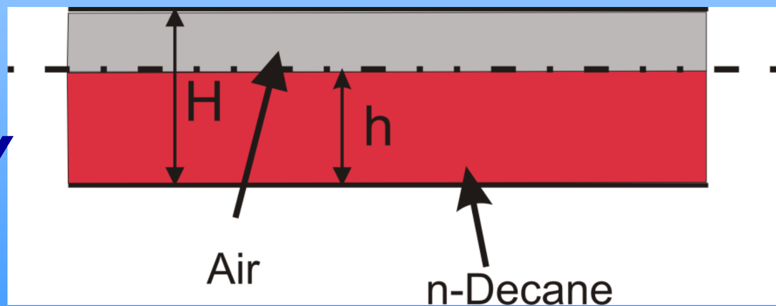

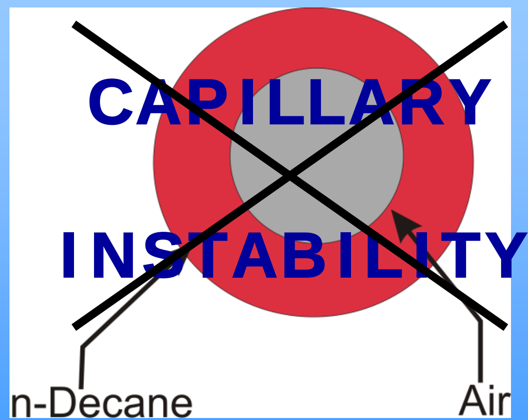

4. Dispersed bubbles cannot appear due to relatively low pressure available; would contradict the observations (reducing liquid flow rate)!

Theoretical Model

$$\frac{d^2u_i}{dy^2} = \frac{1}{\mu_i}\frac{dp}{dx}, \quad i = 1, 2, \qquad \text{..........(1)}$$

The boundary conditions are:

$$y = 0 \quad u_1 = 0; \quad y = H \quad u_2 = 0, \qquad \text{..........(2)}$$

$$y = h \quad u_1 = u_2, \quad \mu_1 \frac{du_1}{dy} = \mu_2 \frac{du_2}{dy}, \qquad \text{..........(3)}$$

where i=1 and 2 correspond to liquid and gas

The Outcome is Amazing!!! Beyond Poiseuille

$$R = \frac{Q_1}{Q_{1,pure}} = -2\bar{h}^3 + 3\frac{\bar{h}^2 - \bar{h}^4(1-\mu_2/\mu_1)}{1-\bar{h}(1-\mu_2/\mu_1)}$$

$$\bar{h} = h/H$$

$$Q_{1,pure} = -H^3/(12\mu_1)dp/dx,$$

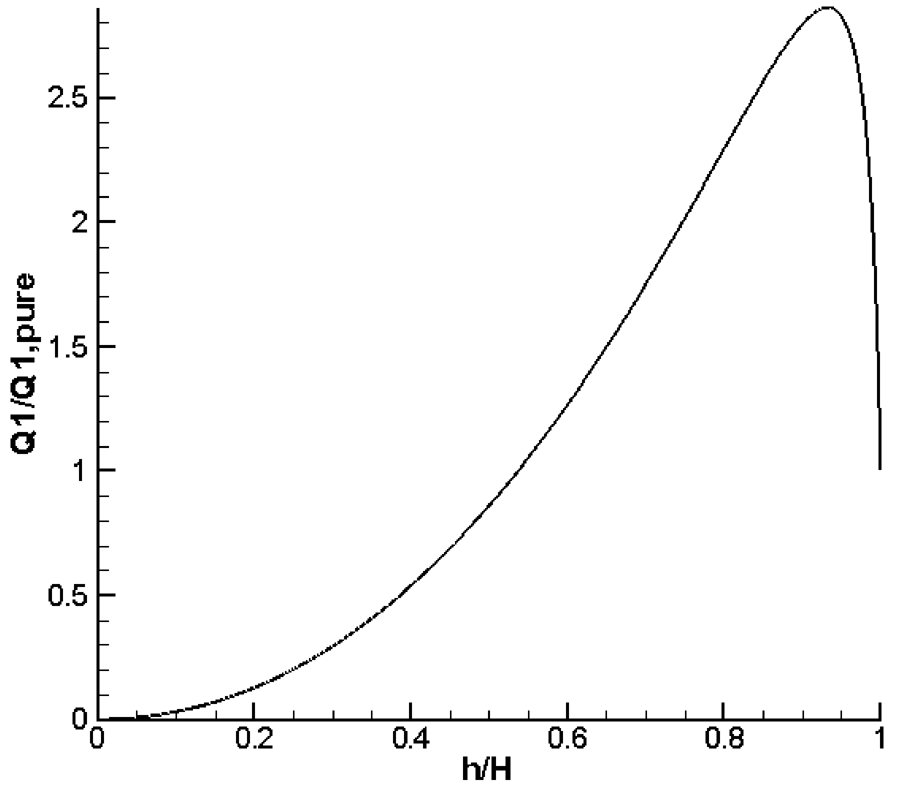

Mechanical & Industrial Engineering

S. Sinha Ray, P. Chando, A.L. Yarin; Nanotechnology 20 (2009) 095711

Explanation

$0.8 \le y / H \le 1$

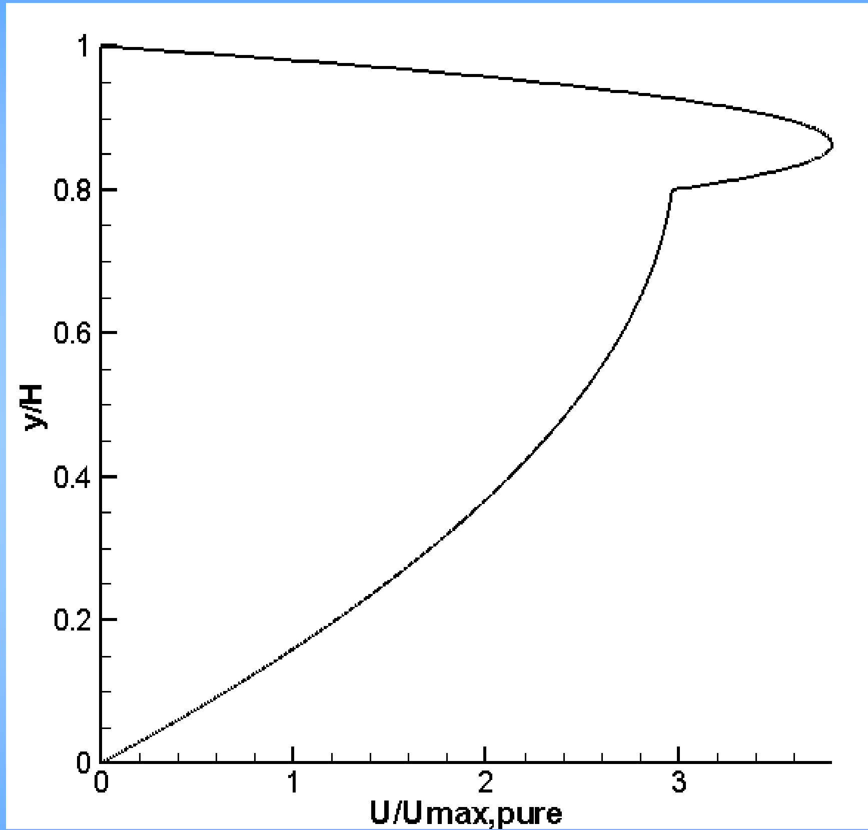

Velocity profile in n-decane/air flow (μ2/μ1=0.0196), h/H=0.8.

Mechanical & Industrial Engineering

Experiments: Observations

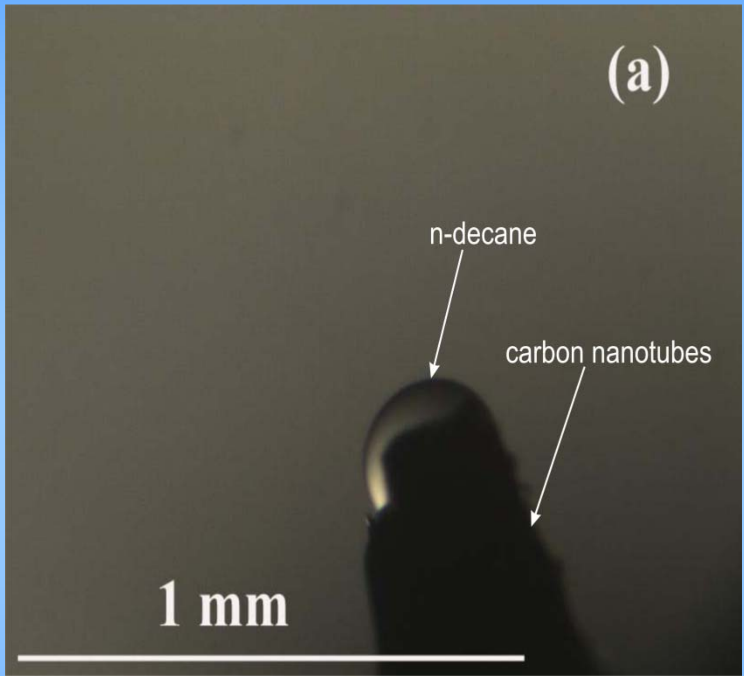

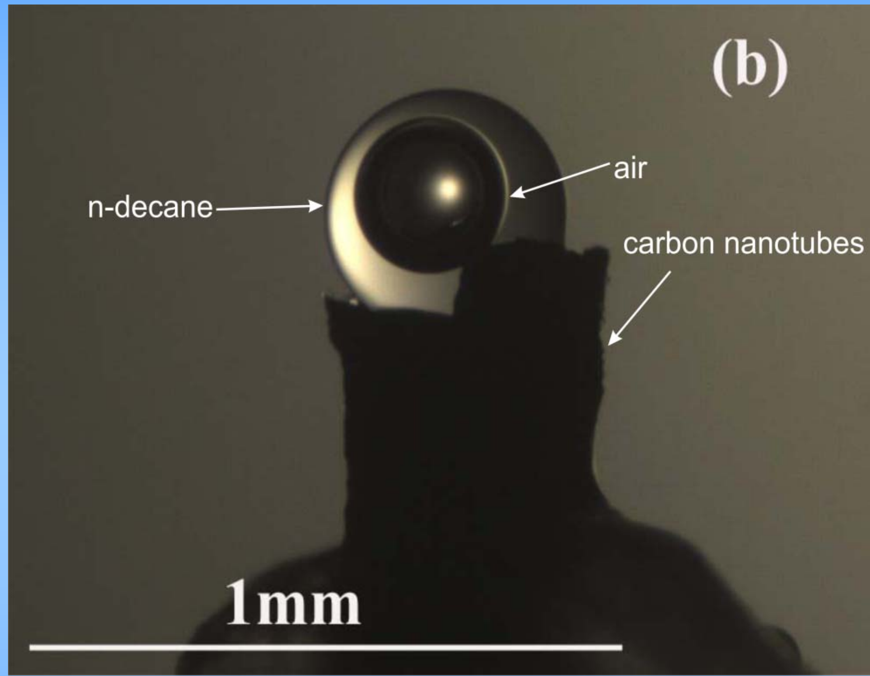

(a) at 1.143 bar **(b) at 1.133 bar**

Same nanotubes at the same pressure

Mechanical & Industrial Engineering

Experiments: Measurements

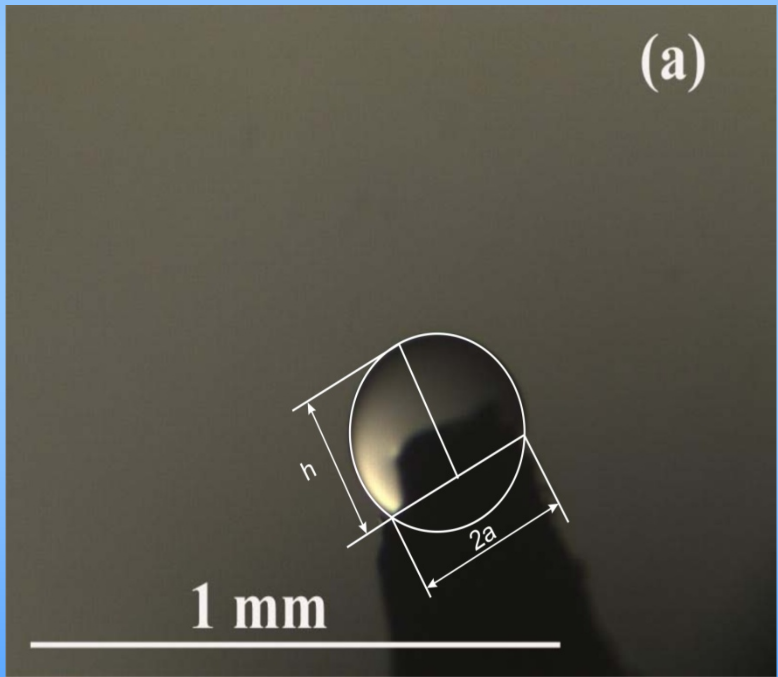

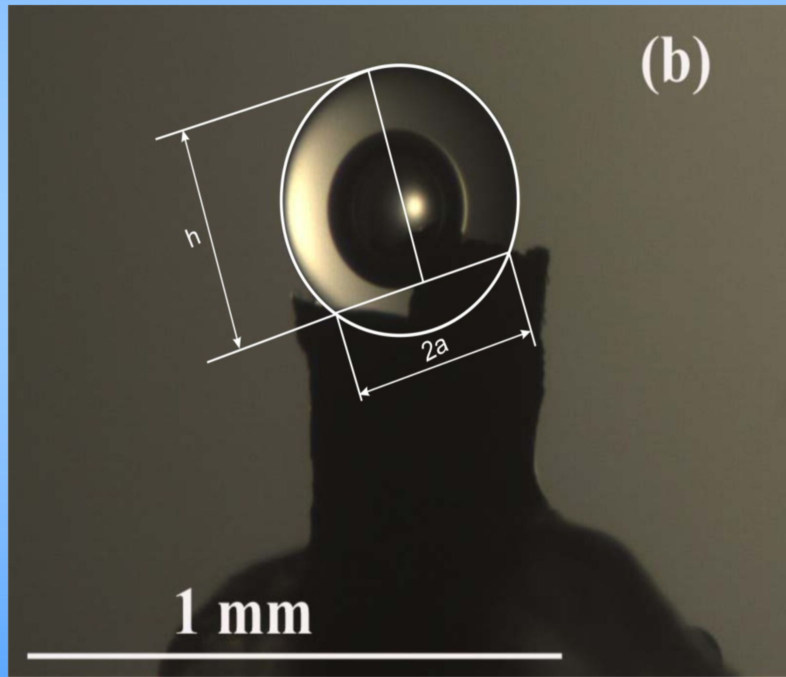

Mechanical & Industrial Engineering

Results

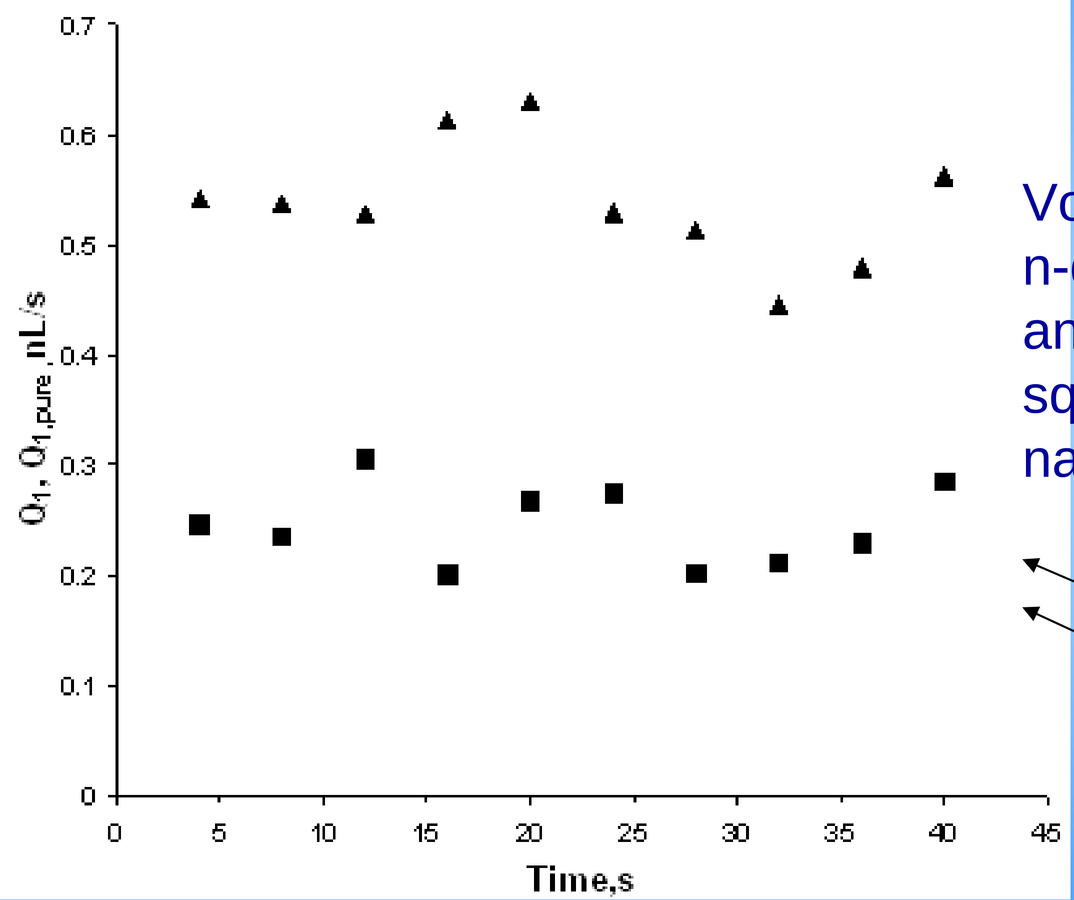

Volumetric flow rates of bi-layer n-decane/air flow (Q_1, triangles) and pure n-decane ($Q_{1,pure}$, squares) through the same carbon nanotube bundle

The average $Q_1 / Q_{1,pure} = 2.188$

Reverse Osmosis for Water Desalination!

Conclusions

(i) **Electrospun nanofiber mats and their metallized or carbonized counterparts (monolithic and hollow) can be used for significant enhancement of heat removal in drop/spray high-heat-flux microelectronics. It is possible to reach heat removal rates of the order of 1 kW/sq.cm with water, which might result in breakthrough in further miniatutrization in microelectroncs devices and computers.**

(ii) **Coelectrospun nanofluidics of layered gas/liquid flows demonstrated how significant benefits for reverse osmosis in water desalination can be achieved.**

Mechanical & Industrial Engineering